Effect of Lithium treatment on SOCE components in Chorea Acanthocytosis

Dissertation

der Mathematisch-Naturwissenschaftlichen Fakultät

der Eberhard Karls Universität Tübingen

zur Erlangung des Grades eines

Doktors der Naturwissenschaften

(Dr. rer. nat.)

vorgelegt von

Basma Sukkar

aus Idleb, Syrien

Tübingen

2019

Gedruckt mit Genehmigung der Mathematisch-Naturwissenschaftlichen Fakultät der Eberhard Karls Universität Tübingen.

Tag der mündlichen Qualifikation:	06.02.2020
Dekan:	Prof. Dr. Wolfgang Rosenstiel
1. Berichterstatter:	Prof. Dr. Peter Ruth
2. Berichterstatter:	Prof. Dr. Friedrich Götz

Acknowledgments

I have the honor to express my deepest sense of gratitude to my supervisor, Prof. Dr. med. Florian Lang for his scholastic guidance and providing all facilities for completion of the research work at the Physiology Institute I, University of Tübingen as well as preparation of this thesis. I am also expressing my heartfelt and sincere gratitude to my second supervisor Prof. Dr. Peter Ruth, who made it possible for me to do the doctorate at the faculty of Mathematics and Natural Sciences with his invaluable cooperation and guidance to review and present my dissertation and to finish my study.

Furthermore, I thank Prof. Dr. Friedrich Götz, for reviewing this dissertation and his great advice to present the dissertation in the final version. I owe as well a dept of gratitude to PD. Dr. Bertolt Gust and PD. Dr. Evi Stegmann for being members of the defense committee and taking this important part in my examination procedure.

My sincere thanks to my colleagues Khalid Nady, Abdulla Al-Mamun Bhuyan, Tamer Al-Maghout, Rashad Tuffaha, Nour Alowayed, Itishri Sahu and Rosi Bissinger for their kind cooperation, suggestions and friendship. I am also grateful to Dr. Lisann Pelzl for her assistance to carry out this research work, as well as all other members of the Physiology Institute I, Tübingen.

My heartfelt thanks to my close friend Duaa Hadid for her continuous support especially during the long work-hours in the institute and the happy times in Tübingen.

I owe my sincere thanks and gratitude to Paul and Rosika Starrach, who were always by my side during my all study time and stay in Tübingen from the very beginning.

As well I would like to say special thanks to Kristina and Karsten Sönnichsen with whom I lived during my study in Tübingen in a very familial atmosphere.

I dedicate this dissertation to my beloved family, mom and dad and my brothers for the unconditional emotional and financial support and continuous blessing which opened the gate and paved the way for my higher studies. My words cannot compensate for their contribution, and this journey would not have been possible without them.

This dissertation is also dedicated to my love and my husband Bassel, who helped me keep up even in difficult times and didn’t lose faith in myself, and who feels like home to my heart...

Sincerely,

Basma Radwan Sukkar

Zusammenfassung

Chorea Acanthocytosis (ChAc) ist eine autosomal rezessive neurodegenerative Erkrankung mit Chorea, Dystonie, Epilepsie und Akanthozytose. Die Patienten haben eine verminderte Lebenserwartung von nur rund 60 Jahren. Die Störung wird durch eine Funktionsverlustmutation des VPS13A Gens (Vacuolar Protein Sortierung - assoziiertes Protein A) verursacht, welches das kodierende Gen für Chorein ist. Normalerweise stimuliert Chorein die Phosphoinositid-3-Kinase (PI3K), die an der Regulation des Ca^{2+} Einstrom beteiligt ist. Veränderungen der intrazellulären Ca2+-Konzentration regulieren unter anderem Proliferation, Differenzierung und Apoptose. Entleerung intrazellulärer Ca^{2+}-Speicher aktiviert den Store-operated Ca^{2+} Entry (SOCE), der durch die Interaktion zwischen dem Ca^{2+}-Sensorprotein, dem Stromal Interacting Molecule 1 (STIM1) und dem porenbildenden Orai1-Kanal zu einer Konformationsänderung und Öffnung des Kanals führt. Der Ca^{2+} Kanal wird auch Ca2+ release activated channel (CRAC) genannt. SOCE wird durch Lithium über Stimulation der Serum & Glukokortikoid-induzierbaren Kinase (SGK1) gesteigert. SGK1 ist in Zellen dafür verantwortlich, die Expression von Orai1 und STIM1 zu stimulieren und ebenfalls den Transkriptionsfaktor Nuclear factor 'kappa-light-chain-enhancer' von aktivierten B-Zellen (NFκB) zu regulieren. Lithium wird unter anderem zur Behandlung von bipolaren Erkrankungen eingesetzt und ist fähig die Bluthirnschranke zu passieren. In dieser Arbeit wurde gezeigt, dass Fibroblasten und Neurone von ChAc-Patienten einen verminderten SOCE und eine erhöhte Apoptoserate besitzen. Fibroblasten wurden von sechs ChAc-Patienten und sechs gesunden Spendern isoliert. Darüber hinaus wurden aus drei weiteren Patienten Fibroblasten entnommen und daraus induzierte pluripotente Stammzellen (iPSCs) erzeugt, um daraus Neurone zu differenzieren. Western Blotting und Calcium-Imaging zeigten eine signifikante Verminderung der Orai1-Proteinmenge bzw. des SOCE in Fibroblasten und iPSC-basierten Neuronen von ChAc-Patienten im Vergleich zu gesunden Spendern. Die RT-PCR zeigte eine signifikante Verminderung der mRNA-Level von Orai1 und STIM1 in iPSC-basierten Neuronen von ChAc-Patienten. Die Apoptose wurde durch Annexin-V/Propidiumjodid-Färbung mittels Durchflusszytometrie nachgewiesen und war bei Fibroblasten und iPSC-basierten Neuronen bei ChAc-Patienten signifikant höher als bei gesunden Spendern.

In dieser Arbeit konnte gezeigt werden, dass die Behandlung der Fibroblasten und Neurone von ChAc-Patienten mit Lithium Calciumsignalwege positiv beeinflusst, während der Orai1-

Blocker, 2-Aminoethoxydiphenylborat (2-APB) den Effekt signifikant reduzierte. Lithium induzierte einen signifikanten Rückgang der Apoptose, der durch 2-APB aufgehoben wurde.
Die mRNA- und Proteinexpression von Orai1 und STIM1 wurde durch Lithium erhöht, aber die Hemmung der SGK1 oder NFκB hat diesen Effekt umgekehrt.
Zusammenfassend lässt sich sagen, dass die apoptotische Wirkung des Choreinmangels bei Fibroblasten und Neuronen von ChAc-Patienten zum Teil auf die verminderte Expression von Orai1, STIM1 und SOCE zurückzuführen war. Die Behandlung mit Lithium konnte diesen Effekt über den SGK1/NFκB Signalweg umkehren, weshalb Lithium eine neue Behandlung der ChAc darstellen könnte.

Abstract

Chorea Acanthocytosis (ChAc) is an autosomal recessive neurodegenerative disease characterized by limb chorea, dystonia, epilepsy and acanthocytosis. The patients have a reduced life expectancy of only around 60 years. This disorder is caused by a loss-of-function mutation of the VPS13A (vacuolar protein sorting-associated protein A) gene, which is the encoding gene of chorein. Normally, chorein stimulates phosphoinositide 3-kinase (PI3K), which is involved in the regulation of Ca^{2+} influx. Oscillations of intracellular Ca^{2+} concentration regulate, among other cell components, proliferation, differentiation and apoptosis. Emptying of intracellular Ca^{2+} stores activates the Store-operated Ca^{2+} entry (SOCE), which leads to a conformational change and opening of the channel through the interaction between the Ca^{2+} concentration sensor protein, the Stromal Interacting Molecule 1 (STIM1), and the pore-forming channel, Orai1. The Ca^{2+} channel is known also as Ca^{2+} release-activated channel (CRAC).

SOCE is increased by lithium via stimulation of serum & glucocorticoid-inducible kinase (SGK1), which is responsible in cells for stimulating the expression of Orai1 and STIM1 as well regulating the transcription factor: Nuclear Factor 'kappa-light-chain-enhancer' of activated B-cells (NFκB). Lithium is used in the treatment of bipolar disorders and can cross the blood-brain barrier (BBB).

In this study, fibroblasts and neurons of ChAc patients have been shown to have decreased SOCE and an increased rate of apoptosis. Fibroblasts were isolated from six ChAc patients and six healthy donors. In addition, fibroblasts were obtained from three additional patients and healthy donors and induced pluripotent stem cells (iPSCs) were generated in order to differentiate them into neurons. Western blotting and calcium imaging showed a significant reduction in the amount of Orai1 protein and SOCE, respectively, in fibroblasts and iPSC-differentiated neurons of ChAc patients compared to healthy donors. RT-PCR showed a significant decrease in the mRNA levels of Orai1 and STIM1 in iPSC-differentiated neurons of ChAc patients. Apoptosis was detected by annexin-V / propidium iodide staining via flow cytometry and was in fibroblasts and iPSC-differentiated neurons of ChAc patients significantly higher than in those of healthy donors.

In this study, it could be shown that the treatment of fibroblasts and neurons of ChAc patients with lithium positively influenced SOCE, an effect significantly reduced by the Orai1

blocker, 2-aminoethoxy diphenyl borate (2-APB). Lithium induced a significant decrease in apoptosis, an effect again abrogated by 2-APB.

The mRNA and protein expression of Orai1 and STIM1 were increased by lithium, an effect reversed by inhibition of SGK1 and NFκB.

In conclusion, the apoptotic effect of chorein deficiency in fibroblasts and neurons of ChAc patients is in part due to the decreased expression of Orai1, STIM1 and SOCE. Treatment with lithium could reverse this effect, via the SGK1/NFκB signaling pathway, which shows that lithium could be a new treatment for Chorea Acanthocytosis.

Table of contents

List of figures

List of tables

Abbreviations

2-APB	2-Aminoethoxydiphenyl borate
Bad	Bcl-2-associated death protein
Bax	Bcl-2-associated X protein
Bcl-2	B-cell lymphoma 2
°C	Degree Celsius
Ca^{2+}	Calcium ion
$[Ca^{2+}]_i$	Cytosolic Calcium concentration
cDNA	Copy deoxyribonucleic acid
ChAc	Chorea Acanthocytosis
CRAC	Calcium release-activated channel
CRACM	Calcium release-activated channel modulator
DMEM	Dulbecco's modified Eagle Medium
DMSO	Dimethyl sulfoxide
EGTA	Ethylene glycol-bis(β-aminoethyl ether)-N,N,N',N'-tetraacetic acid
ER	Endoplasmic Reticulum
FACS	Fluorescence-activated cell sorting
FBS	Fetal Bovine Serum
FITC	Fluorescein isothiocyanate
Foxo3a	forkhead box class O transcription factor 3a
Fwd	Forward
GAPDH	Glyceraldehyde 3-phosphate dehydrogenase
GSK-3	Glycogen synthase kinase 3
HRP	Horseradish peroxidase
I_{CRAC}	Calcium release-activated channel current
iPSCs	Induced pluripotent stem cells
MDM	Murine double minute
ml	Milliliter
mM	Millimolar
µM	Micromolar
NFκB	Nuclear factor κ light chain enhancer of activated B cells
nM	Nanomolar

PBS	Phosphate buffered saline
PCR	Polymerase chain reaction
PI3K	Phosphoinositide 3-kinase
Rev	Reverse
RNA	Ribonucleic acid
RT	Room temperature
SDS	Sodium dodecyl sulfate
SDS-PAGE	Sodium dodecyl sulfate polyacrylamide gel electrophoresis
SGK1	Serum and glucocorticoid-inducible kinase 1 or Serine/threonine-protein kinase 1
SOCE	Store-operated Ca^{2+} entry
SR	Sarcoplasmic Reticulum
STIM	Stromal Interacting Molecule
TBS	Tris-buffered saline
TBST	Tris-buffered saline (TBS) containing 1% Tween 20
TEMED	N,N,N’N’-Tetramethylethylenediamine

1. Introduction

1.1 Chorea Acanthocytosis (ChAc)

1.1.1 Background, diagnosis and therapy

Chorea Acanthocytosis (ChAc) is a fatal neurodegenerative disease characterized by red blood cell acanthocytosis and loss of striatal neurons as a hallmark like other neurodegenerative diseases (Jung et al., 2011). It progresses to cause premature death of the patient (Jung et al., 2011). Autosomal-recessive ChAc is caused by a loss-of-function mutation in the vacuolar protein sorting 13 homolog A (VPS13A) gene leading to a lack of the functional respective encoded protein chorein (Velayos-Baeza et al., 2004, Dobson-Stone et al., 2004).

This disease could be diagnosed by several procedures. The first diagnostic step for ChAc is to evaluate the levels of muscle creatine kinase (CK), as well the serum concentrations of liver enzymes lactate dehydrogenase (LDH), alanine transaminase (ALT) and aspartate transaminase (AST) which have shown to be increased in ChAc patients (Velayos Baeza et al., 1993). The molecular genetic diagnosis of the disorder will be by sequencing the gene VPS13A. This gene is located on the long (q) arm of chromosome 9 at the position 21.2 (9q21,2) and it is relatively a big gene of 73 exons which has two main splice forms or transcripts: transcript A (exons 1-68 and 70-73), and transcript B (exons 1-69) (Rampoldi et al., 2001, Dobson-Stone et al., 2004). Expression of transcript A in full exons is required for a full-length chorein (Dobson-Stone et al., 2004). The big size of the VPS13A gene makes the screening for mutations is a hefty and time-consuming procedure to reach the right diagnosis of Chorea Acanthocytosis, therefore an easier diagnostic method could be the cellular detection of chorein by western blot analysis of patient erythrocytes, which shows a missed chorein protein band in patients samples and thus gives an early indication of the disorder, a differential diagnosis that will not be found in patients of Huntington’s disease or McLeod syndrome (Dobson-Stone et al., 2004) (Figure 1).

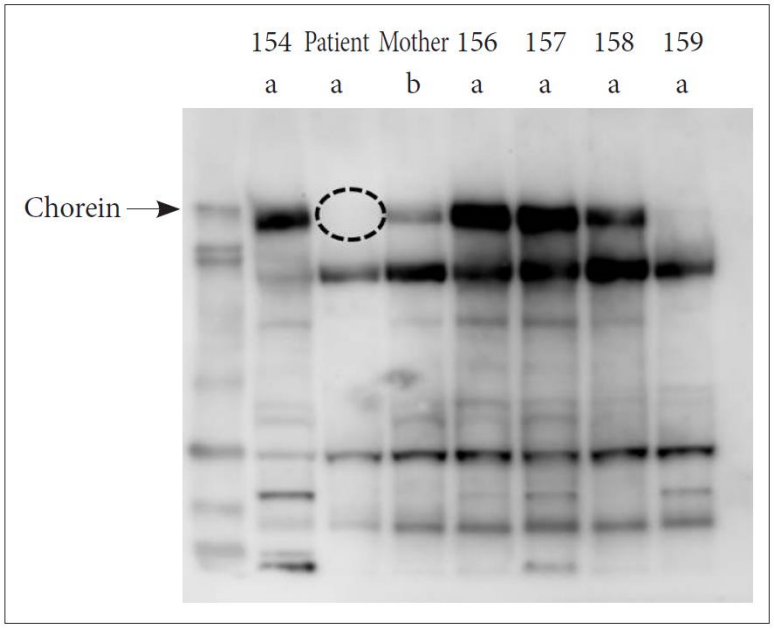

Figure 1: Absence of chorein protein.
Western blot demonstrating the absence of chorein protein band in a sample from ChAc patient. The figure is used after permission from (Walker, 2015).

The blood of most ChAc patients will contain a highly variable percentage of acanthocytes, between 5%-50% of the red blood cell population (Rampoldi et al., 2002) (Figure 2).

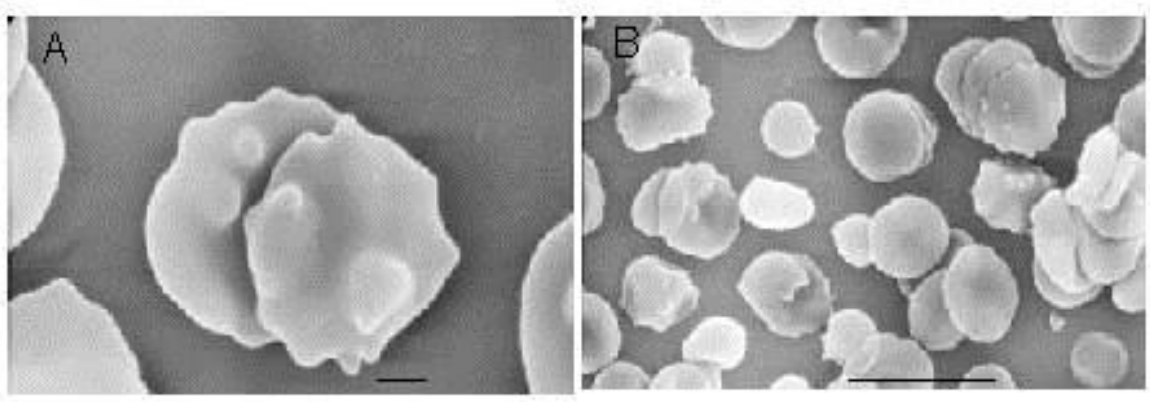

Figure 2: Acanthocytosis in the blood of ChAc patient.
Scanning electron microscopy of erythrocytes from ChAc patient's peripheral blood that shows the presence of acanthocytosis (scale bar in A: 1 µm; in B: 10 µm). The figure is used after permission from (Zhang et al., 2013).

On the other hand, the clinical characteristics could give also a certain diagnose of the disorder; which include dystonia that will affect the oral region and tongue especially, as tongue and lip biting that, in turn, leads to dysarthria and dysphagia and ends with weight loss (Bader et al., 2010). Other clinical diagnostic features include seizures and epilepsy (Scheid et al., 2009), myopathy, characterized by distal muscle wasting and weakness and

amyotrophy, subtle eye movement abnormalities and movement disorder as limb chorea (Velayos Baeza et al., 1993).

The current treatment of Chorea Acanthocytosis is only symptomatic and supportive, as Botulinum toxin injections for relaxing the muscles and to control the oro-lingual dystonia (Schneider et al., 2006) and other drugs to relieve the psychiatric and movement symptoms (Velayos Baeza et al., 1993).

1.1.2 Chorein and its role

Chorein is a large protein, more than 3000 amino acids with a predicted molecular weight of 360 kDa (Ueno et al., 2001, Dobson-Stone et al., 2004), expressed highly in tissues like testis, kidney, spleen and brain and less in lungs, liver and placenta (Kurano et al., 2007, Ueno et al., 2001) as well in many cell types including vascular endothelial cells (Alesutan et al., 2013), neuronal cells (Hayashi et al., 2012), platelets (Schmidt et al., 2013), erythrocytes and skin fibroblasts (Dobson-Stone et al., 2004).

It has essential roles in the cell, and many cellular functions are chorein-sensitive such as, dopamine release (Honisch et al., 2015a), endothelial cell stiffness (Alesutan et al., 2013), cytoskeletal architecture (Honisch et al., 2015b) and survival of tumor cells, neurons and skeletal muscle cells (Velayos Baeza et al., 1993, Saiki et al., 2007, Honisch et al., 2015c).

Furthermore, chorein has a function on regulation the secretion and aggregation of blood platelets according to a previous study which showed that lack of chorein in platelets of ChAc patients leads to significantly reducing the expression of vesicle-associated membrane protein 8 (VAMP8), an important protein for secretion of platelets granules (Polgar et al., 2002, Schmidt et al., 2013).

In a previous study, erythrocytes of ChAc patients showed a decreased level of phosphorylation of the p21 protein-activated kinase 1 (PAK1) and depolymerization of cortical actin, which reflects the role of chorein on regulation cytoskeletal architecture (Foller et al., 2012, Honisch et al., 2015b). Moreover, chorein silencing resulted in decreasing the phosphorylation of Bcl-2-associated death protein (Bad) and this led to prompt apoptosis by causing the mitochondrial depolarization as well DNA fragmentation and exposure of phosphatidylserine at the cell surface, all hallmarks for apoptosis, which confirm the effect of chorein in cell survival (Foller et al., 2012).

According to proteome analysis, there was found a binary protein-protein interaction between chorein and phosphoinositide-3-kinase (PI3K) (Wu et al., 2007, European Molecular Biology Laboratory, 2011), moreover, lack of chorein leads to decreased level of the activation and phosphorylation of p85 subunit of phosphoinositide-3-kinase (PI3K) (Foller et al., 2012).
The PI3K plays a crucial role in many critical pathways for cell survival and cell growth which are both sensitive to Ca^{2+} signaling (Orrenius et al., 2003, Burgoyne, 2007, Vanhaesebroeck et al., 2012). The next parts will describe the mechanism of this crucial signaling pathway, its role and how does this kinase affect Ca^{2+} signals.

1.2 Calcium signaling

1.2.1 Importance and basics

Intracellular calcium is known as one of the most important cellular signals in many mechanisms such as fertilization, cell motility, gene transcription, secretion, apoptosis and necrosis (Berridge, 1993, Carafoli, 2002, Berridge et al., 2003). In neuronal functions as particular, Ca^{2+} signaling has a dominant role in gene expression, neuronal growth, neurotransmission, survival and death (Orrenius et al., 2003, Burgoyne, 2007).
The system of Ca^{2+}-signaling has a basic common component in all cell types, that to perform brief pulses between external medium and intracellular store using a pack of molecules that work together to achieve the signal (Berridge et al., 2000, Berridge et al., 2003).
Ca^{2+} could be released from its intracellular stores, the endoplasmic reticulum (ER) or the sarcoplasmic reticulum (SR), as a reaction to many stimulants (Koch, 1990, Berridge, 1993). These stimulants, such as insulin or growth factors, when interacting with cell surface receptors, for example, G protein-coupled receptors (GPCRs) or receptor of tyrosine kinases (RTKs), induce the activation of two important players in the process of Ca^{2+} release, phospholipase Cγ (PLCγ) and PI3K (Rhee and Bae, 1997, Katan, 1998, Bootman et al., 2002, Putney and Tomita, 2012, Vanhaesebroeck et al., 2012). After activation, PLCγ and PI3K work in related pathways: On the one hand, activation of PLCγ leads to hydrolysis the signaling lipid phosphatidylinositol 4,5-bisphosphate (PtdIns-4,5-P2) (PIP_2) to form diacylglycerol (DAG) and inositol-1,4,5-triphosphate (In3P) (Clapham, 1995). In3P then binds to its receptor, inositol-1,4,5-triphosphate receptors (In3PR), on ER and triggers the release of calcium (Clapham, 1995). On the other hand, when PI3K is activated, it

phosphorylates (PIP_2) into phosphatidylinositol-3,4,5-trisphosphate (PtdIns-3,4,5-P3) (PIP3) which in turn feeds back to enhance again the PLCγ to catalyze the breakdown of PIP2 to In3P and DAG (Scharenberg and Kinet, 1998).

Calcium enters into the cell by a capacitative mechanism, i.e. when the intracellular stores of calcium are empty, this sends a signal to the membrane of the cell and activates calcium influx in order to refill the stores (Putney, 1986, Takemura et al., 1989). This signal was understood after the finding of Stromal Interacting Molecule 1 (STIM1) which was described as the sensor of calcium in the ER (Roos et al., 2005, Liou et al., 2005), and the other player to complete the mechanism was Orai1-3, the pore-forming subunit of calcium channels in the cellular membrane (Feske et al., 2006, Vig et al., 2006b, Zhang et al., 2006). Capacitative calcium entry and Store-operated calcium entry (SOCE) are two names of one mechanism.

Hoth and Penner also explained that depletion of calcium stores leads to an electrophysiological inward current, highly selective to calcium, and caused by activation of Ca^{2+} channels, which they called calcium release-activated calcium current (I_{CRAC}) (Hoth and Penner, 1992).

1.2.2 STIM1

STIM1 was known and described at first as a tumor suppressor gene (Parker et al., 1996), until the demonstration of Roos et al., and Liou et al. at 2005 that STIM1 is a component of homeostasis for Ca^{2+} signals (Roos et al., 2005, Liou et al., 2005). In Drosophila S2 cells there was found a single Stim gene (dstim) (Roos et al., 2005), but in mammalian HeLa cells were two human homologs found for dstim, STIM1 and STIM2 (Liou et al., 2005). The physiological function of STIM2 is controversial as it didn't show the same effect on I_{CRAC} in all cell lines (Putney, 2007).

STIM1 is composed of 685 amino acids and is located in the membrane of the ER via a transmembrane domain, that when Ca^{2+} concentration is low, a conformational change acts on the domains and causes the I_{CRAC} activation (Roos et al., 2005, Liou et al., 2005, Zhang et al., 2005b).

STIM1 molecule has three coiled-coil domains: the intracellular C terminal contains the second and third coiled-coil domains which make together the so-called; CRAC activating domain (CAD) as it is responsible to activate the Orai1 channel (Park et al., 2009), while the domain in the luminal of ER is at the N-terminal and contains a signal peptide that senses the

concentration of Ca^{2+} in the ER store leading to a change in the structure of STIM1 domains, and results in oligomerization of several STIM1 molecules followed by activation of SOCE (Liou et al., 2005, Zhang et al., 2005b, Soboloff et al., 2006, Stathopulos et al., 2006, Mercer et al., 2006, Wu et al., 2006) (Figure 3).

The C-terminus has also the CRAC modulatory domain (CMD) that senses the negative response to Ca^{2+} influx and leads to stopping the activation of Orai1 channel and inactivation of I_{CRAC} (Park et al., 2009).

1.2.3 Orai1

Feske et al described Orai1 as a crucial Ca^{2+} channel for I_{CRAC} (Feske et al., 2006). This was proved by the genetic mapping of severe combined immunodeficiency (SCID) patients whose I_{CRAC} was defective, which showed a mutation in the Orai1 protein that caused the hydrophobicity of the channel, and led to the defective I_{CRAC} (Feske et al., 2006). On the other hand, knockdown of dstim and dorai in Drosophila induced complete inhibition of I_{CRAC} (Feske et al., 2006).

In Drosophila, dorai was identified and had three human homologs, Orai1, Orai2 and Orai3, or CRACM1, CRACM2, CRACM3 as they were also named (Feske et al., 2006, Vig et al., 2006b, Zhang et al., 2006). Orai2 and Orai3 function like Orai1 but their Ca^{2+} currents are smaller and sometimes undetectable (Mercer et al., 2006). This was noticed after overexpression of STIM1 with Orai2 or Orai3 which resulted in either a slight increase or no effect on I_{CRAC} (Mercer et al., 2006).

The Ca^{2+} channel is made up of Orai1 tetramer (Ji et al., 2008, Mignen et al., 2008, Penna et al., 2008). Orai1 is a protein of 301 amino acids consists of four transmembrane domains (TM) located in the plasma membrane and connected by one intracellular and two extracellular loops with its N and C terminus are in the cytoplasm (Hou et al., 2012). The N- and C- terminus of Orai1 are both important for the activity of the channel and they both have the functional binding sites for activated STIM1 (Muik et al., 2008, Palty et al., 2015). Never the less, the C-terminus of Orai1 binds to STIM1 stronger than N-terminus, and deleting the C-terminus will barrier Orai1 from interacting with STIM1 (Muik et al., 2008). The N-terminus contains a calmodulin binding domain (CBD) (Mullins et al., 2009) which is important for the mechanism calcium-dependent inactivation (CDI) to keep cytosolic Ca^{2+} concentration low when the cell is at the resting situation (Roos et al., 2005) (Figure 3).

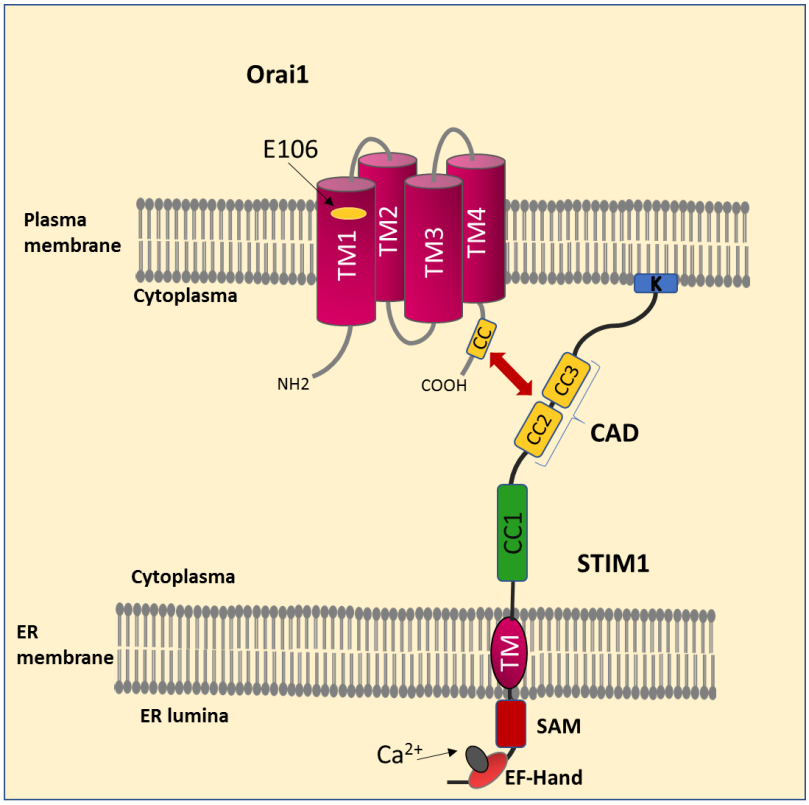

Figure 3: Model of Orai1 and STIM1.

Orai1 has four transmembrane domains (TM), with its N- and C- terminus localized in the cytoplasm and involves two extracellular loops and one intracellular loop; the TM1 has the glutamic acid 106 (E106) which is identified as the Ca^{2+}-binding amino acid and the selectivity filter of the CRAC channel (Prakriya et al., 2006, Vig et al., 2006a, Gwack et al., 2007, McNally et al., 2009, Zhou et al., 2010). The intracellular C-terminus includes the coiled-coil (CC) domain, which binds to STIM (Li et al., 2007, Muik et al., 2008, Yuan et al., 2009). STIM1 has one transmembrane domain in the ER membrane. The N-terminus has Ca^{2+} binding EF-hand domain that represents the sensor of Ca^{2+} concentration in the ER and interacts with the SAM (sterile alpha motif) domain to result in the oligomerization of several STIM1 molecules (Stathopulos et al., 2006, Luik et al., 2008, Muik et al., 2011). The C-terminus contains the CRAC activation domain (CAD) that interacts with Orai1and activates the CRAC channel, and the end of the C-terminus has lysine (K) -rich domain which allows the interaction with plasma membrane lipids (PIP2) and (PIP3) (Liou et al., 2007, Feske et al., 2012). Figure adapted from (Feske et al., 2012), changed.

1.2.4 Formation of I_{CRAC}

When STIM1 senses the depletion of Ca^{2+} in the ER by its N-terminal luminal domain, this results in the conformational change of STIM1 into oligomers (dimers, tetramers…) followed by its migration to be near the plasmatic membrane and binding to the C terminus of Orai1. Then Orai is pulled to form the puncta between ER and plasma membrane, which ends with opening Orai1 channel by its N-terminus followed by Ca^{2+} entry into the ER (Liou et al., 2005, Hogan et al., 2010) (Figure 4).

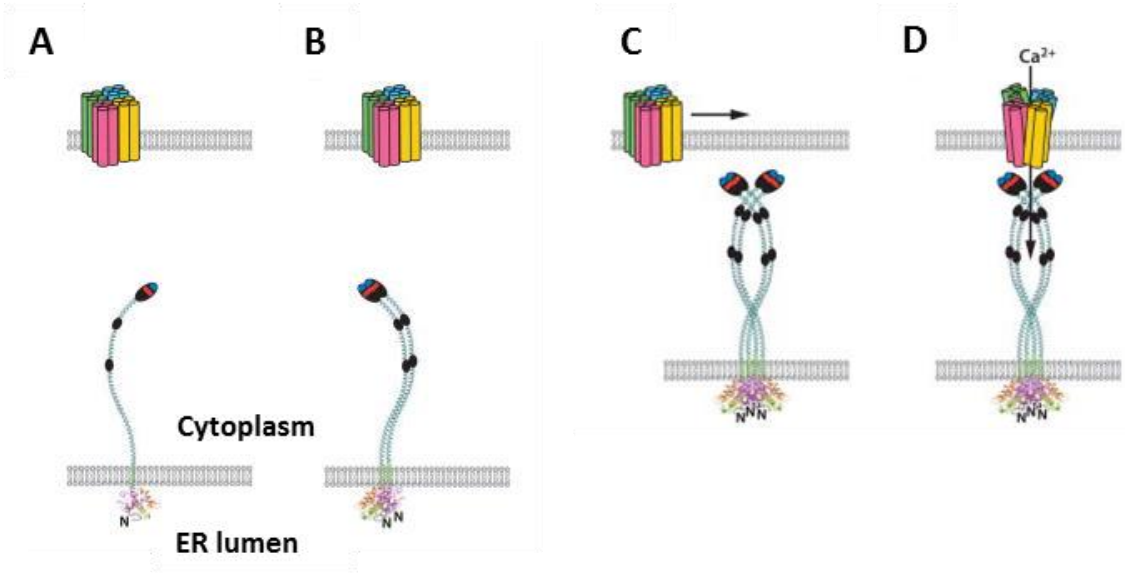

Figure 4: Steps of store-operated Ca^{2+} entry.

(A) Resting state where STIM1 is a monomer, Orai1 as an oligomer (probably a tetramer) and ER Ca^{2+} stores are filled with Ca^{2+}, (B) ER Ca^{2+} stores are depleted and STIM1 oligomerization starts and forms oligomers (dimers for example), (C) migration of STIM1 to ER-plasma membrane appositions and binding the STIM1 lysin (K)-rich regions to lipids in the plasma membrane, as well, STIM1 oligomers bind to the C-terminal of Orai1 and recruit it to the ER-plasma membrane junctions, (D) Orai1 channel is opened and Ca^{2+} enters the cell (Li et al., 2007, Muik et al., 2008, Park et al., 2009, Yuan et al., 2009, Kawasaki et al., 2009, Muik et al., 2009, Hogan et al., 2010). Figure adapted from (Hogan et al., 2010), changed.

1.3 Effect of lithium on cell survival and neurodegenerative diseases

Lithium is one of the oldest psychiatric treatments since the 19th and till now, and its benefits were known for reducing the risk of suicide and mortality in mood disorders as mania (Cade, 1949), aggressive behavior (Sheard et al., 1976, Muller-Oerlinghausen and Lewitzka, 2010) depression (Crossley and Bauer, 2007) and bipolar disorder (BD) (Alda, 2015).

It also batters neurodegeneration in many diseases such as Huntington's disease, Parkinson's disease, Alzheimer's disease, amyotrophic lateral sclerosis (Alvarez et al., 2002, Lazzara and Kim, 2015, Bauer et al., 2003) and spinocerebellar ataxias type 1 and 3 (Watase et al., 2007).

The plasma levels that were needed for a full clinical effect of lithium is between 0.6 and 1 mmol/L (Alda, 2015).

The importance of lithium comes from its beneficial effects on basic characters of mood and neurodegenerative disorders reducing neuronal excitability and neuronal death.

On the one hand, lithium ions reduce the resting membrane potential and neuronal excitability, which increases during the episodes of the illness, by reducing intracellular sodium and calcium via voltage-gated sodium channels (Schou, 1957, Huang et al., 2007, Gao et al., 2010).

On the other hand, it has a neuroprotective effect achieved by many mechanisms: Lithium can inhibit glycogen synthase kinase-3 (GSK-3) at concentrations 1-2 mM either directly, by competition for a magnesium-binding site with GSK-3, or indirectly by Akt (serine/threonine kinase or protein kinase B as also known) activation which leads to further inhibiting the proapoptotic forkhead box class O transcription factor (Foxo3a), Bcl-2-associated death protein (Bad) and murine double minute (MDM) (Jope, 1999, Beaulieu et al., 2004, Avila et al., 2012, Lazzara and Kim, 2015). Another mechanism is by regulating pro-apoptotic proteins as Blc-2-associated X protein (Bax), which binds and antagonizes Bcl-2 protein to prompts apoptosis, and the tumor suppressor protein p53 which targets both Bcl-2 and Bax and promotes cell death (Lazzara and Kim, 2015, Basu and Haldar, 1998). Lithium also activates the up-regulation of brain-derived neurotrophic factor (BDNF) which boosts the survival and plasticity of neurons (McAllister et al., 1999, Lazzara and Kim, 2015), in addition, it increases the levels of Bcl-2 protein which provide the anti-apoptotic activity (Youdim and Arraf, 2004). Moreover, lithium is able to be an anti-oxidant as it increases the levels of GSH in neurons, the glutathione that decreases when oxidative stress occurs in the

neurons and leads to increase the cellular levels of hydrogen peroxidase and thus induces cell death (de Vasconcellos et al., 2006, Kim et al., 2011).

1.4 Aim of the study

The aim of this study is to understand the pathophysiology of Chorea Acanthocytosis (ChAc) and to test if it is paralleled with neuronal regulation of Ca^{2+} release-activated Ca^{2+} channels Orai1, and/or its regulator STIM1 in order to identify potential therapeutic targets for the treatment of ChAc.

After the success that lithium has shown on neuroprotection and reducing mortality in bipolar disease, Alzheimer's disease and Parkinson's disease, the hypothesis was if lithium will have the same protecting effect on Chorea Acanthocytosis and could be a therapy for these patients.

The experiments were performed on fibroblasts and iPSC-differentiated neurons from ChAc patients and were compared with samples from healthy donors to:

- Understand the pathophysiology of Chorea Acanthocytosis
- As SOCE is an important player in cell protection, would it be affected or play a role in Chorea Acanthocytosis?
- Would lithium be a possible therapy to protect neuronal and cell death in Chorea Acanthocytosis?

2. Materials

2.1 Chemicals

Name	Company name and country of origin
30% Acrylamide Mix	Carl Roth, Karlsruhe, Germany
Ammonium persulfate	Carl Roth, Karlsruhe, Germany
Bio-Rad Protein Assay Dye Reagent	Bio-Rad, München, Germany
Calcium chloride ($CaCl_2$)	Sigma Aldrich, St. Louis, USA
Chloroform	Carl Roth, Karlsruhe, Germany
Developer and Replenisher	Kodak, USA
DMEM (1X) + GlutaMax™ -1	Gibco, Paisley, UK
DMSO	Carl Roth, Karlsruhe, Germany
Dulbecco's Phosphate Buffered Saline (DPBS)	Sigma-Aldrich, St. Louis, USA
EGTA	Roth, Karlsruhe, Germany
Ethanol 99%	Carl Roth, Karlsruhe, Germany
Fetal calf serum (FCS)	Thermo Fisher Scientific, Waltham, Massachusetts
Fixer and Replenisher	Kodak, USA
Fura-2/AM	Invitrogen, Goettingen, Germany
Glucose	Sigma Aldrich, St. Louis, USA
Glycine	Carl Roth, Karlsruhe, Germany
GSK-650394	Sigma-Aldrich, St. Louis, USA
Isopropyl alcohol	Carl Roth, Karlsruhe, Germany
Lithium chloride	Sigma-Aldrich, St. Louis, USA
Magnesium sulfate ($MgSO_4$)	Sigma Aldrich, St. Louis, USA
Methanol	Sigma-Aldrich, St. Louis, USA
Non-fat milk powder	Carl Roth, Karlsruhe, Germany
Penicillin/Streptomycin	Invitrogen, Karlsruhe, Germany
PeqGold protein marker	PeqLab, Erlangen, Germany
PeqGold TriFast	PeqLab, Erlangen, Germany
PMSF	Sigma-Aldrich, St. Louis, USA
Potassium chloride (KCl)	Carl Roth, Karlsruhe, Germany

RIPA lysis buffer	Cell Signaling Technology, USA
Roti®-Load 1 (4x)	Carl Roth, Karlsruhe, Germany
SDS	Carl Roth, Karlsruhe, Germany
Sodium chloride (NaCl)	Carl Roth, Karlsruhe, Germany
Sodium hydrogen phosphate (Na_2HPO_4)	Roth, Karlsruhe, Germany
Roti®-Free Stripping Buffer	Carl Roth, Karlsruhe, Germany
TEMED	Carl Roth, Karlsruhe, Germany
Thapsigargin	Invitrogen, Darmstadt, Germany
Tris-base	Carl Roth, Karlsruhe, Germany
Trypsin-EDTA	Gibco, Paisley, UK
Tween 20	Carl Roth, Karlsruhe, Germany
Wogonin hydrate	Sigma-Aldrich, St. Louis, USA

2.2 Antibodies

Antibody	**Source**	**Manufacturer**
Anti-GAPDH antibody	Rabbit	Cell Signaling Technology, USA
Anti-Orai1 antibody	Rabbit	Cell Signaling Technology, USA
Anti-STIM1 antibody	Rabbit	Cell Signaling Technology, USA
Anti-rabbit HRP-conjugated antibody		Cell Signaling Technology, USA

2.3 Primers

Gene	**Sequence**
Orai1 – fwd	CGTATCTAGAATGCATCCGGAGCC
Orai1 – rev	CAGCCACTATGCCTAGGTCGACTAGC
STIM1 – fwd	CCTCGGTACCATCCATGTTGTAGCA
STIM1 – rev	GCGAAAGCTTACGCTAAAATGGTGTCT
GAPDH – fwd	TGAGTACGTCGTGGAGTCCAC
GAPDH – rev	GTGCTAAGCAGTTGGTGGTG

2.4 Kits

GoScript™ Reverse Transcription System	Promega, Hilden, Germany
GoTaq® qPCR Master Mix	Promega, Hilden, Germany

ECL detecting reagents	Amersham, Freiburg, Germany
eBioscience™ Annexin V Apoptosis Detection Kit FITC	Thermofisher Scientific, San Diego, USA

2.5 Solutions and Buffers

Table 1. Resolving gel (10%)

Component volumes (ml) per 5 ml gel mold volume	
H_2O	1.9
30% Acrylamide Mix	1.7
1.5 M Tris (pH 8.8)	1.3
10% SDS	0.05
10% ammonium persulfate	0.05
TEMED	0.002

Table 2. Stacking gel (5%)

Component volumes (ml) per 1ml gel mold volume	
H_2O	0.68
30% Acrylamide Mix	0.17
1.0 M Tris (pH 6.8)	0.13
10% SDS	0.01
10% ammonium persulfate	0.01
TEMED	0.004

Table 3. Running buffer (10X)

Tris base	250 mM
Glycine	1.9 M
SDS	1%
dH2O	Up to 1 liter

Table 4. Transfer buffer

Tris base	198 mM
Glycine	1.5 M
dH2O	Up to 1 liter

Table 5. TBS (10X)

Tris base	200 mM
NaCl	1.3 M
dH2O	Up to 1 liter, pH 7.6

TBS 1X was prepared using dH2O and 1% Tween 20 was added to get at the end TBST 1X.

Table 6. Standard Ringer solution (pH 7.4)

Components in mM:	
NaCl	125
KCl	5
$MgSO_4$	1.2
$CaCl_2$	2
Na_2HPO_4	2
HEPES	32
Glucose	5
d.H_2O	To reach 1 liter

Table 7. Ca^{2+}-free Ringer solution (pH 7.4)

Components in mM:	
NaCl	125
KCl	5
$MgSO_4$	1.2
Na_2HPO_4	2
HEPES	32
EGTA	0.5
Glucose	5
d.H_2O	To reach 1 liter

2.6 Equipment

Name	Company name and country origin
Amersham hyper film	GE Healthcare, München, Germany
Agarose gel electrophoresis chamber	BioRad, München, Germany
Axiorvert 100	Carl Zeiss, Oberkochen, Germany
BioPhotometer	Eppendorf, Hamburg, Germany
Borosilicate glass pipettes	Harvard Apparatus, UK
CFX96 real-time system	Bio-Rad Laboratories, Germany
Cuvettes, Uvette	Eppendorf AG, Germany
DMZ puller	Zeitz, Augsburg, Germany
Electrophoresis and blotting system	Bio-Rad Laboratories, Germany
EPC 9 amplifier	Heka, Lambrecht, Germany
Pipette 0,5/10, 10/100, 100/1000	LABMATE Optima, Germany
Flow cytometry machine, FACS Calibur™	BD Biosciences, USA
Heraeus cell culture hood	Thermo Fisher Scientific, USA
Heraeus cell culture incubator	Thermo Fisher Scientific, USA
Amersham Hyperfilm™ ECL	GE Healthcare Limited, UK
MS31 electrical micromanipulator	MW, Märzhäuser, Wetzlar, Germany
Vortex	Scientific Industries, USA
Pipette man, pipetus®	Hirshmann Laborgerate, Germany
pH meter	Sartorius, Göttingen, Germany
Corning® Costar® Stripette® serological pipettes 5, 10, 25 ml	Corning Incorporated, Corning NY, USA
SterileTubes 15, 50 ml	Greiner bio-one, Germany
Sterile Tips 10, 100, 200, 1000 µl	Biozyme, USA
Cell Culture plate 6, 12, 24, 96 well	Costar, USA
Tissue Culture Flask 75ml	SARSTEDT, Germany
qPCR 96 well plate	Peqlab, Erlangen, Germany

3. Methods

3.1 Cells

The study has been approved by the Ethical Commission of the University of Tübingen (598/2011) and by the Institutional Review Board of the Technische Universität Dresden (EK45022009). Informed consent was obtained from all participants and/or their legal guardian/s.

3.1.1 Isolation of fibroblast from skin biopsies

Skin biopsies were isolated from ChAc patients (n=6) and healthy donors (n=6). The biopsies were minced by sterile techniques, washed twice in PBS supplemented with antibiotics (100 U/ml penicillin and 100 mg/ml streptomycin) and cultivated in fibroblast medium DMEM (Biochrom, Berlin, Germany) supplemented with 10% FCS and antibiotics (100 U/ml penicillin and 100 mg/ml streptomycin) and maintained at 37°C in a humidified atmosphere of 5% CO_2 and 95% air until fibroblast grew out of the biopsy. To detach the established fibroblasts, trypsin 0.25% and 0.05% EDTA were used for 5 min and the separated cells were aliquoted and the aliquots were cultured again with the same previously described medium. Cells between passage three and twelve were used for the study.

3.1.2 Generation of induced pluripotent stem cells (iPSCs)

The generation of iPSCs was according to the published protocol (Okita et al., 2011).
Fibroblasts were obtained from additional patients (n=3) and healthy donors (n=3) (see 3.1.1). $1x10^5$ of fibroblasts were electroporated using (Nucleofector 2D, Lonza) with a total of 1 µg per plasmid which carries the sequences for hOCT4, hSOX2, hKLF4, hL-MYC, and hLIN28. After electroporation, fibroblasts were cultivated in fibroblast medium DMEM + 10% FBS for 1 day, and then the medium was supplemented with 2 ng/ml fibroblast growth factor FGF-2 (Peprotech). From day 3 on, cells were cultivated in Essential 8 (E8) medium containing 100 µM Na-butyrate (NaB) (Sigma-Aldrich). After 3 – 4 weeks, the iPSC colonies were picked manually and expanded in Matrigel-coated 6-well plates. At passage 7 – 10,

iPSCs were characterized and frozen in E8 medium supplemented with 40% KOSR (Thermo Fisher Scientific), 10% DMSO (Sigma-Aldrich) and 1 µM Y-27632 (Selleckchem, Munich, Germany).

A careful characterization of the generated iPSCs and the establishment of a robust and reliable protocol to generate neurons is important to provide consistent phenotypes. For this purpose, genomic and functional validation was applied to the generated cells. The genomic validation was done using the exclusion of plasmid-integration, SNP array analysis for genetic integrity and resequencing of mutation site, and the functional validation was applied via confirmation of expression of pluripotency marker and verification of the *in vitro* differentiation potential using a protocol yielding ß-III-tubulin/CTIP-2 positive neurons as described in (Hauser et al., 2016).

3.1.3 Neuronal differentiation and treatment of iPSCs

To generate cortical neurons, the previously described protocol was used (Shi et al., 2012). To achieve the neural conduction of iPSCs, dual SMAD inhibitors (10 µM SB431542 (Sigma-Aldrich) and 500 nM LDN-193189 (Sigma-Aldrich)) were added to the 3N medium. After 10 days, cells were collected and expanded by cultivation in 3N medium supplemented with 20 ng/ml FGF-2 for 2 days. From day 12 on, cells were cultivated in 3N medium with a medium change every other day. Cell culture was passaged on day 27 and re-plated appropriately for the specific assay. (RNA/Protein isolation & Flowcytometry: $5x10^5$ cells per cm^2; Ca^{2+} measurements: $5x10^4$ cells per cm^2; Patch clamp: $2.5x10^5$ cells per cm^2).

3.2 Treatments

Where indicated, treatment with lithium was done by LiCl solution and cells were treated with 2mM. Wogonin and GSK650394 were solved in DMSO and cells were treated with (50 µM) and (10 µM) respectively. The solvent did not influence the effects that were studied.

3.3 Quantification of mRNA expression

3.3.1 RNA isolation

Cells were lysed in 500 µl TriFast reagent. 200 µl chloroform was added, heavily mixed and incubated in RT for 3 min, then centrifuged at 12000 x g for 15 min at 4°C. The upper layer was transferred into a new eppendorf tube and mixed with 250 µl ice-cold Isopropanol and incubated for 10 min in RT. The mixture was centrifuged at 12000 x g for 10 min at 4°C. After this step the RNA pellet becomes visible and the supernatant was carefully removed. 500 µl of 70% ice-cold Ethanol was added to wash the pellet then centrifuged at 7000 x g for 5 min at 4°C. The supernatant was carefully removed, and the pellet was left to air dry for 30 min in RT then resuspended in 15 µl of RNase-free water for 15 min at 55°C.
The concentration of the RNA samples was measured using BioPhotometer at λ260 and λ280 after dilution 1:69 in RNase-free water.

3.3.2 cDNA synthesis

The synthesis was performed using the GoScript™ Reverse Transcription System (Promega) according to the manufacturer protocol. After DNase digestion, the volume of 2 µg RNA was completed with RNase-free water to reach the volume 10 µl, then 1 µl random primers and 1 µl oligonucleotides where added and the mix was incubated at 70°C for 5 min, chilled directly in 4°C and 4 µl GoScript™ 5X Reaction Buffer, 2 µl of $MgCl_2$, 1 µl PCR Nucleotide Mix and 1 µl GoScript™ Reverse Transcriptase was added, mixed and incubated at 25°C for 5 min, 42°C for 60 min and followed with 70°C for 15 min to inactivate the reverse transcriptase. Samples were then either saved at - 20°C or proceeding to the next step.

3.3.3 Quantitative PCR

Real-time polymerase chain reaction (RT-PCR) was performed to determine the transcript levels of the respective genes. The total reaction mix volume was 15 µl and contained: 1.5 µl of cDNA, 7.5 µl of 2x GoTaq® qPCR Master Mix (Promega), 1.5 µl forward and reverse primer mix and 4.5 µl nuclease-free water. Then amplification was performed in 96 well plates on a CFX96 Real-Time System (Bio-Rad) as the following program:

1- 95°C for 5 min
2- 95°C for 10 sec.
3- 58°C for 20 sec.
4- 72°C for 25 sec + Plate read
5- GOTO 2, 40 more times
6- 95°C for 10 sec.
7- Melt curve: 60°C to 95°C, increment 0,2°C for 5 sec + Plate read

The Data were analyzed using the $\Delta\Delta C_T$ method and the house-keeping gene GAPDH was used as an internal control to standardize the mRNA levels of the sample.

3.4 Protein abundance quantification

3.4.1 Protein lysate

The cells were cultured in 6 well plates and treated for the right time accordingly, then 200 µl/well Trypsin (incubated in 37°C water bath for 15 min) was added to cells and incubated in 37°C for 5 min. Then 500 µl/well PBS was added, and the cells were collected in eppendorf 1.5 ml tubes, centrifuged (1000 rpm, 5min, Rt) and the pellet was washed twice in PBS and then re-suspended in 40 µl ice-cold RIPA lysis buffer containing 1 mM PMSF (Sigma Aldrich) and kept in ice for 30 min, This protein lysate was stored in - 80°C or proceeded with the next steps.

3.4.2 Protein concentration determination

The protein concentration was measured using the Bradford assay (Bio-Rad). For this purpose, 2 µl from the protein lysate was mixed with 1 ml of diluted Bradford buffer (the Bradford buffer was diluted with distilled H_2O 1:5), then the concentration was measured at λ595 by the Photometer. The Photometer was calibrated to measure absorbance till 1, and so if any sample gave an absorbance over this range, it was diluted with RIPA lysis buffer containing 1 M PMSF.

3.4.3 SDS polyacrylamide gel electrophoresis

With the usage of SDS-PAGE, the proteins could be separated according to their molecular weight (Laemmli, 1970). And for this result, 100 µg protein were solubilized in Laemmli sample buffer (Roti Loading Dye) and cooked at 95°C for 5 min. The gels were prepared (as described in Tables 1 and 2) in the gel cassettes (Electrophoresis and blotting system, Bio-Rad) and the samples were loaded in the wells of the gel. To allocate the right protein size, Protein-Marker VI (Peqlab) was loaded in the gel also. The samples were separated by using a running buffer (see Table 3) at a voltage of 80 V, and when the proteins were concentrated, the voltage was raised to 100 V.

3.4.4 Blotting and protein detection

The proteins were electro-transferred by 100 V onto nitrocellulose membranes for 90 min in transfer buffer (see Table 4), and this step was chilled using ice blocks located in the transfer tank (Electrophoresis and blotting system, Bio-Rad). The membranes were washed with TBST 1X (see Table 5) and then blocked with 5% fat-free milk (Carl Roth) solved in TBST for 1 h at RT, then incubated with primary antibody (1:1000 in 1% fat-free milk solved in TBST) at 4°C overnight. After incubation, the blots were washed with TBST for 5 min, 3 times at RT, then incubated with the anti-rabbit HRP-conjugated secondary antibody (1:2000, in 1% fat-free milk solved in TBST) for 1 h at RT. Additional washes with TBST were applied on the blots for 5 min, 3 times at RT, then the protein bands were detected using ECL detection reagents and quantified with Quantity One Software (BioRad, München, Germany) or *ImageJ*.

In some cases, the same blot was used to check more than one antibody, and for that purpose, the blot was washed, after the first detection, with Roti®-Free Stripping Buffer (Carl Roth) at 57°C for 30 min, then washed and then incubated with the other wanted primary antibody and the same previous protocol was followed.

3.5 Ca^{2+} measurements

To measure the cytosolic Ca^{2+} concentration ($[Ca^{2+}]_i$), Fura-2 fluorescence was used.
Cells were loaded with 2 µM of Fura-2/AM (Invitrogen) for 20-45 min at 37°C. Second, a Ringer standard solution (see Table 6) was added to the cells for 3 min and the cells were excited at λ_{340} and λ_{380} through an objective (Fluor 40x/1.30 oil) related to an inverted fluorescence microscope (Axiovert 100). Emitted fluorescence intensity was recorded at λ_{505}, and data were acquired every 10 seconds using specialized computer software (Metafluor, Universal Imaging, Downingtown, USA). Then to determine SOCE; a Ca^{2+}-free Ringer solution (see Table 7) was added to achieve Ca^{2+}-free conditions for 3 min, following comes a depletion of intracellular Ca^{2+}-stores using 1 µM of sarco-endoplasmic reticulum Ca^{2+}-ATPase inhibitor, thapsigargin (Bird et al., 2008), then Ca^{2+} was added again using the Ringer standard solution.
To quantify Ca^{2+} entry, the slope (delta ratio/s) and peak (delta ratio) were calculated after Ca^{2+} re-addition.

3.6 Cell death estimation

A normal cell has a phosphatidylserine (PS) layer located in the inner layer of the cell membrane, and in apoptosis, the cell membrane becomes ruptured, which enables Annexin to enter and bind to PS (Reutelingsperger and van Heerde, 1997, Elmore, 2007). On the other hand, in necrotic cell death, the plasma membrane becomes permeable as the nucleic membrane, this makes it possible that nucleic acid dyes, such like propidium iodide (PI) to bind to the DNA and gives its red fluorescence giving a quantification of necrotic or late apoptotic cells (Darzynkiewicz et al., 1997).
We used a combination of the PS marker, annexin, with the nuclear dye, PI, to detect apoptotic and necrotic cells by flow cytometry, and the chemicals of the experiment were

from the kit eBioscience™ Annexin V Apoptosis Detection Kit FITC (Thermofisher Scientific).

For this purpose, cells were incubated and treated in 12 well plates, then washed from the medium with 200 µl PBS, centrifuged at 1000 rpm for 5 min, then washed with 200 µl of 1X annexin washing buffer (AWB), centrifuged and the supernatant trashed. Staining was done using 50 µl of AWB containing 1 µl of Annexin V-FITC (Immunotools, Friesoythe, Germany) and incubated in dark in 37°C for 15 min. Then 150 µl of AWB was added to the cells, the plate was centrifuged, and the supernatant was discarded. After that, the PI staining was applied using 200 µl of (AWB) containing 2 µl of PI (Bioscience, Germany) and then incubated in dark and 37°C for 8-10 min. After incubation, 200 µl of AWB was added and annexin V-FITC, as well as PI fluorescence, was determined by flow cytometry using FACS Caliber (BD, Heidelberg, Germany).

Statistics

Data are expressed as arithmetic means ± SEM. Statistical analysis was done by unpaired t-test or ANOVA, and results with $p < 0.05$ were considered as statistically significant.

4. Results

4.1 Effect of ChAc on Orai1 abundance

To start the work, Orai1 abundance was compared between fibroblasts of healthy and ChAc patients. Thus, after isolating and preparation of fibroblasts from both healthy donors and ChAc patients starting from skin biopsies isolation and reaching the step when fibroblasts were ready to use, the protein abundance of Orai1 was quantified using western blotting (see 3.4). Protein was isolated from fibroblasts, separated using SDS-PAGE, and transferred onto nitrocellulose membrane and incubated with Orai1 antibody. GAPDH was used as a control to uniform the loading of the samples on the gel. And then the membrane was incubated with a secondary HRP-conjugated antibody. The results showed that Orai1 protein abundance in fibroblasts isolated from ChAc patients was significantly lower than in fibroblasts isolated from healthy donors (Figure 5).

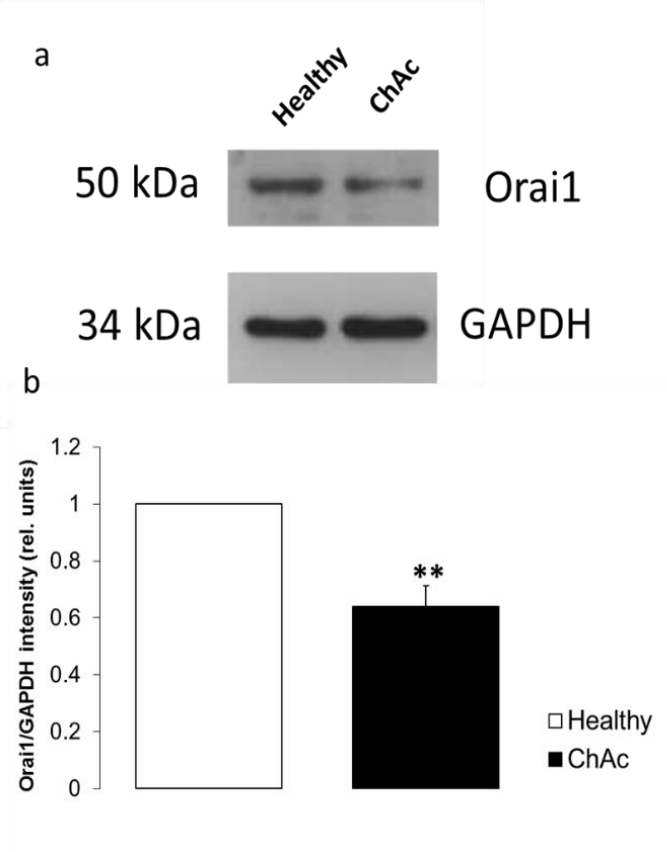

Figure 5: Orai1 protein abundance in fibroblasts isolated from healthy donors and ChAc patients.
(a) Original western blot of Orai1 protein abundance in Fibroblasts isolated from healthy donors and ChAc patients. (b) Arithmetic means (±SEM, n=5 healthy donors and 5 patients) of Orai1 protein abundance in isolated fibroblasts from healthy donors (white bar) and ChAc patients (black bar).
** $p<0.01$ indicates a statistically significant difference compared to the respective value in fibroblasts isolated from healthy donors. Figure adapted from (Pelzl et al., 2017a), changed.

4.2 Influence of chorein deficiency on intracellular Ca^{2+} release and store-operated calcium entry (SOCE)

Lack of functional Orai1 will affect SOCE (Feske et al., 2006). For checking, Fura-2 fluorescence was used to measure the cytosolic Ca^{2+} activity ($[Ca^{2+}]_i$) (see 3.5). First, Ca^{2+}-free solution was applied to the cells, then to deplete intracellular Ca^{2+} stores, a Ca^{2+}-free solution containing (1µM) thapsigargin, which is a sarco-endoplasmic reticulum Ca^{2+} ATPase (SERCA) inhibitor, was added, and this led to a rapid transient increase in intracellular Ca^{2+} activity $[Ca^{2+}]_i$ similar in both control fibroblasts and healthy fibroblasts (Figure 6). Following was the re-addition of extracellular Ca^{2+} during the maintained presence of thapsigargin, and this resulted in a rapid increase of Fura-2 fluorescence in both, healthy control and ChAc fibroblasts referring to store-operated Ca^{2+} entry (SOCE) (Figure 6). As shown in (Figure 6), the peak of SOCE in fibroblasts isolated from ChAc patients was significantly lower than in fibroblasts isolated from healthy donors.

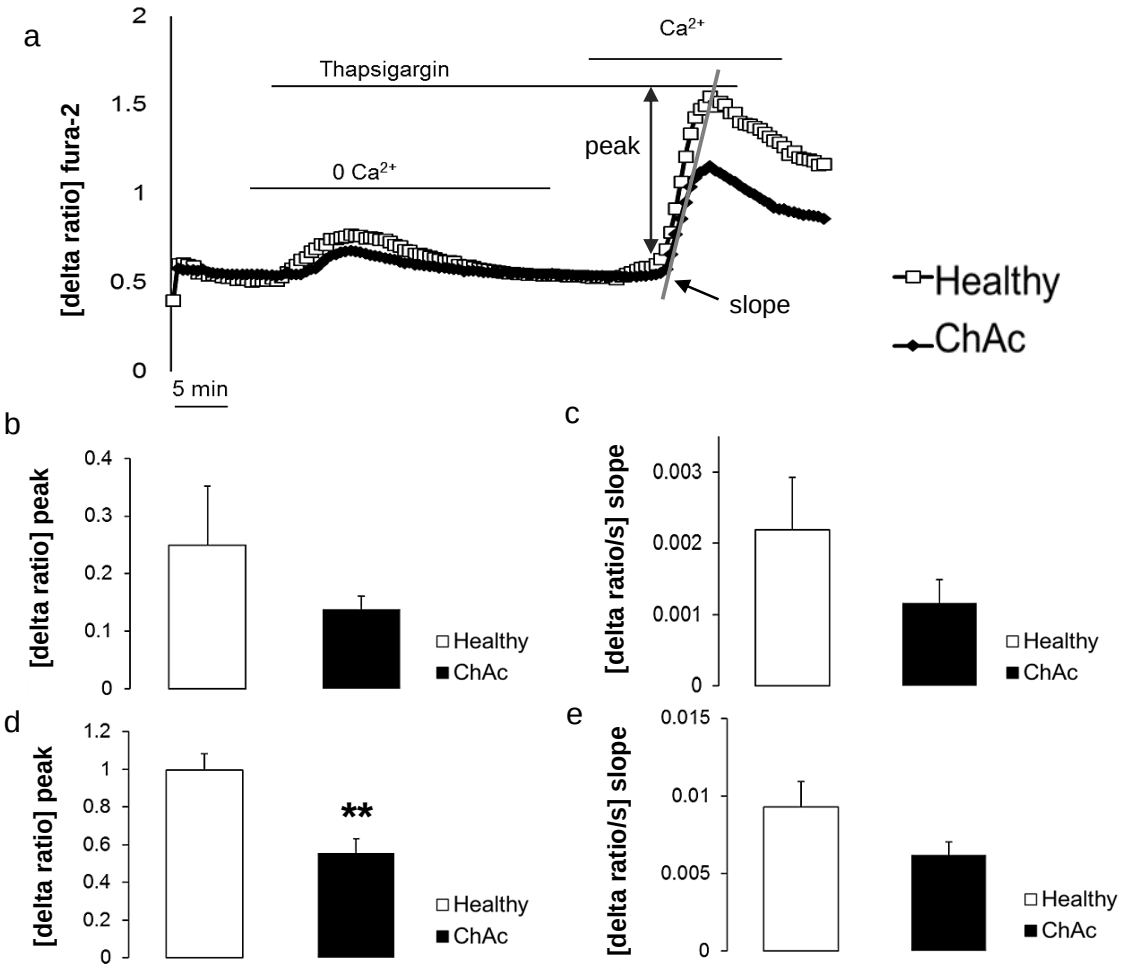

Figure 6: Difference of intracellular Ca^{2+} release and store-operated Ca^{2+} entry in fibroblasts isolated from healthy donors and ChAc patients.

(a) Representative tracings of Fura-2 fluorescence-ratio in fluorescence spectrometry during Ca^{2+}-free conditions with the presence of thapsigargin (1 µM), and then after re-addition of extracellular Ca^{2+} in fibroblasts isolated from healthy donors and ChAc patients. (b,c) Arithmetic means (±SEM, n=48-61 cells from 4-5 individuals) of peak (b) and slope (c) increase of Fura-2 fluorescence-ratio after the addition of thapsigargin into Ca^{2+}-free conditions in fibroblasts isolated from healthy donors and ChAc patients. (d,e) Arithmetic means (±SEM, n=48-61 cells from 4-5 individuals) of peak (b) and slope (c) increase of Fura-2 fluorescence-ratio after the re-addition of extracellular Ca^{2+} in fibroblasts isolated from healthy donors and ChAc patients. ** $p<0.001$ indicates a statistically significant difference compared to the respective value in fibroblasts isolated from healthy donors. Figure adapted from (Pelzl et al., 2017a), changed.

4.3 Lithium treatment restores SOCE in fibroblasts isolated from ChAc patients

To explore the validity of the hypothesis about lithium, fibroblasts isolated from ChAc patients were treated with lithium (24 hours, 2 mM) and then Fura-2 fluorescence-ratio was employed to check if there will be any difference on intracellular Ca^{2+} activity or store-operated Ca^{2+} entry (SOCE) (see 3.5). Exposure of the cell to Ca^{2+}-free solution containing thapsigargin (1 µM), the sarco-endoplasmic reticulum Ca^{2+}/ATPase (SERCA) inhibitor, was used to deplete intracellular Ca^{2+} stores. This leads to an increase of intracellular Ca^{2+} activity which was significantly higher in ChAc patients-isolated fibroblasts treated with lithium (24 hours, 2 mM) than untreated ChAc fibroblasts (Figure 7). Then re-addition of extracellular Ca^{2+} in the continued presence of thapsigargin gave a rapid increase of Fura-2 fluorescence reflecting SOCE, which was in fibroblasts treated with lithium (24 hours, 2 mM) again significantly higher than untreated ChAc fibroblasts (Figure 7).

To go deeper, fibroblasts were treated with Orai1 blocker 2-Aminotheoxydiphenyl Borat (2-APB) (50 µM) together with lithium (2 mM) for 24 hours and the results showed that both slope and peak of SOCE in fibroblasts isolated from ChAc patients were significantly decreased by 2-APB treatment (Figure 7).

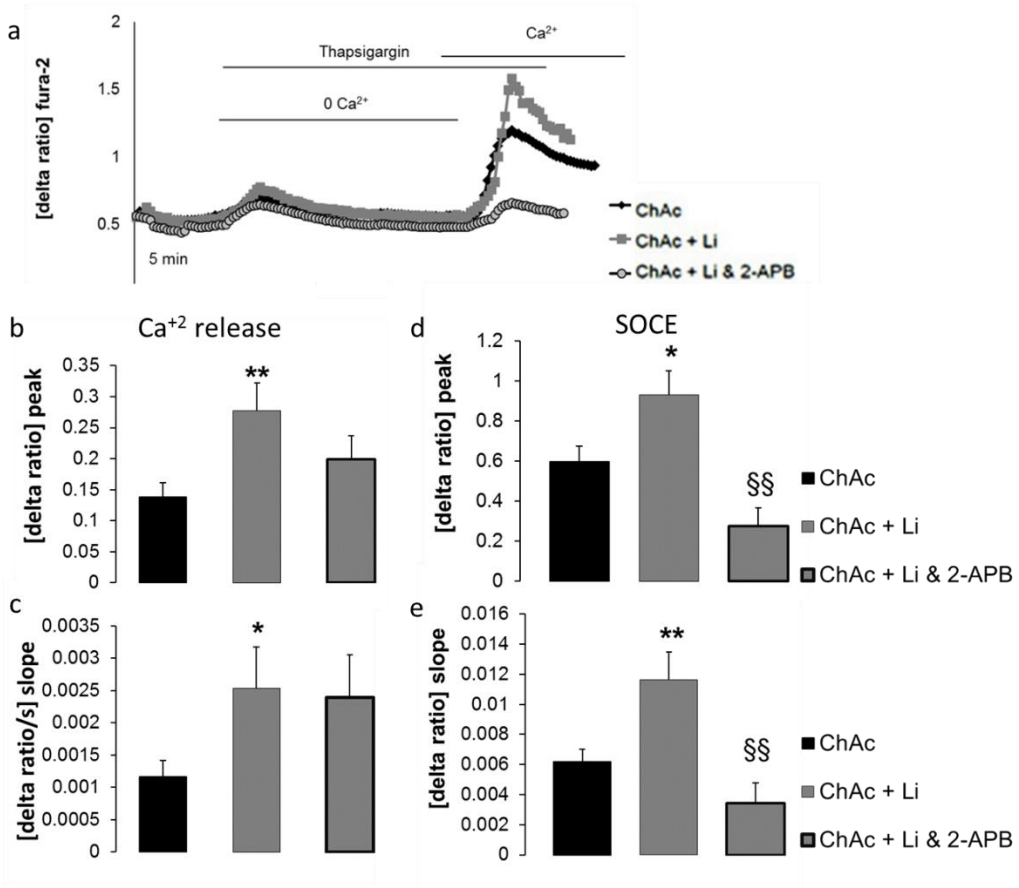

Figure 7: Effect of lithium treatment on fibroblasts isolated from ChAc patients without and with additional treatment with Orai1 blocker 2-APB.

(a) Representative tracings of Fura-2 fluorescence-ratio in fluorescence spectrometry before and after removal of extracellular Ca^{2+} and depletion of intracellular Ca^{2+} stores by thapsigargin (1 µM) and then followed by re-addition of extracellular Ca^{2+} in the continued presence of thapsigargin in fibroblasts isolated from ChAc patients untreated or treated with lithium (24 hours, 2 mM) alone or treated with both lithium (2 mM) and 2-APB (50 µM) together for 24 hours. (b,c) Arithmetic means (±SEM, n=23-73 cells from 4-5 individuals) of peak (b) and slope (c) increase of Fura-2 fluorescence-ratio after the addition of thapsigargin (1µM) in fibroblasts isolated from ChAc patients without treatment or treated with lithium (24 hours, 2 mM) alone or treated with both lithium (2 mM) and 2-APB (50 µM) together for 24 hours. (d,e) Arithmetic means (±SEM, n=23-73 cells from 4-5 individuals) of peak (d) and slope (e) increase of Fura-2 fluorescence-ratio after the re-addition of extracellular Ca^{2+} in fibroblasts isolated from ChAc patients without treatment or treated with lithium (24 hours, 2 mM) alone or treated with both lithium (2 mM) and 2-APB (50 µM) together for 24 hours. * $P<0.05$, ** $p<0.01$ indicates a statistically significant difference compared to the respective value of untreated ChAc fibroblasts. §§ $p<0.01$ indicates a statistically significant difference compared to the respective value of ChAc fibroblasts treated with lithium alone. Figure adapted from (Pelzl et al., 2017a), changed.

4.4 Effect of chorein deficiency on the survival of fibroblasts isolated from healthy donors and ChAc patients

To test if the difference in Ca^{2+} signaling between healthy and ChAc fibroblasts is paralleled by differences in apoptosis also, flow cytometry quantification was used (see 3.6).

To identify phosphatidyl exposing cells, annexin-V-binding was utilized, while propidium iodide was used to identify cells with the permeable cell membrane. The results showed that the percentage of annexin-v-binding fibroblasts that are isolated from ChAc patients was significantly higher than the percentage of annexin-V-binding fibroblasts that are isolated from healthy donors (Figure 8). Furthermore, the percentage of propidium iodide-stained cells changed between healthy and ChAc fibroblasts, and this percentage was in fibroblasts isolated from ChAc patients significantly higher than healthy donors' fibroblasts (Figure 8).

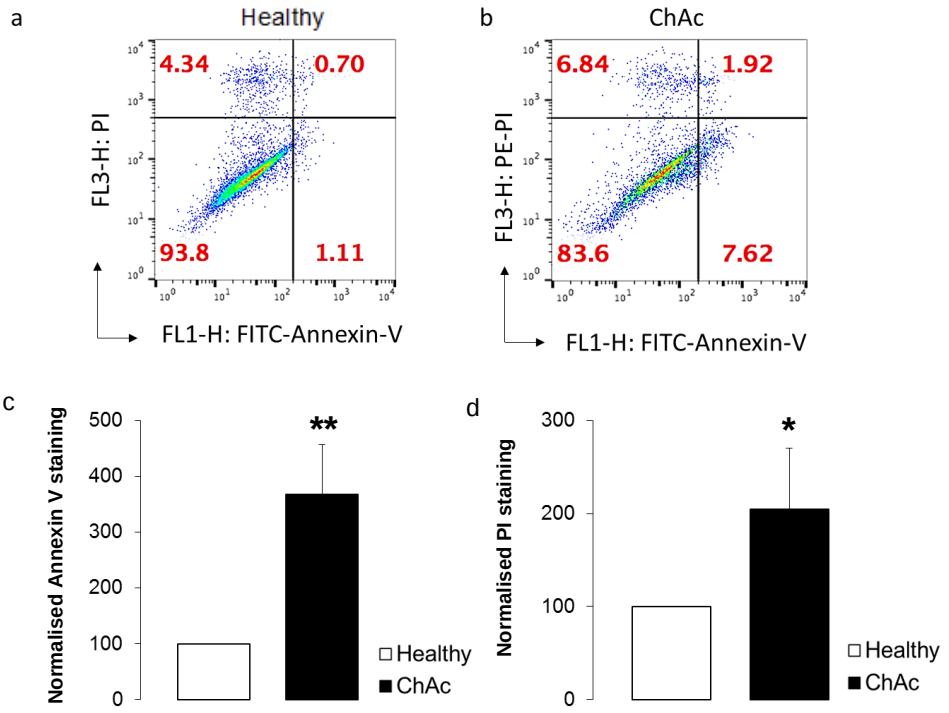

Figure 8: difference in phosphatidylserine translocation and propidium iodide uptake between fibroblasts isolated from healthy donors and fibroblasts isolated from ChAc patients.

(a,b) Representative dot blots of propidium iodide harboring versus annexin-V- binding in fibroblasts isolated from healthy donors and ChAc patients. (c) Arithmetic means (± SEM, n=4-5 individuals) of annexin-V-binding fibroblasts isolated from healthy donors and from ChAc patients and both expressed in the percentage of the value in healthy donors. (d) Arithmetic means (± SEM, n=4-5 individuals) of propidium iodide harboring fibroblasts isolated from healthy donors and from ChAc patients and both expressed in the percentage of the value in healthy donors. * $p<0.05$, ** $p<0.01$ indicates a statistically significant difference compared to the respective value in fibroblasts isolated from healthy donors. Figure adapted from (Pelzl et al., 2017a), changed.

4.5 Lithium treatment leads to survival of fibroblasts isolated from ChAc patients

To explore if the lithium treatment will make any difference in isolated fibroblasts apoptosis, again phosphatidylserine translocation utilizing annexin-V-binding and propidium iodide uptake was measured. As a result, after lithium (24 hours, 2mM) treatment on fibroblasts isolated from ChAc patients, the percentage of annexin-V-binding fibroblasts as well propidium iodide harboring fibroblasts decreased significantly compared to untreated

fibroblasts. Treatment of fibroblasts isolated from ChAc patients with Orai1 blocker 2-APB (50µM), increased significantly the percentage of both, annexin-V-binding and propidium iodide staining. Treatment with both lithium and 2-APB didn't result in a significant decrease in annexin-V-binding or propidium iodide staining fibroblasts (Figure 9).

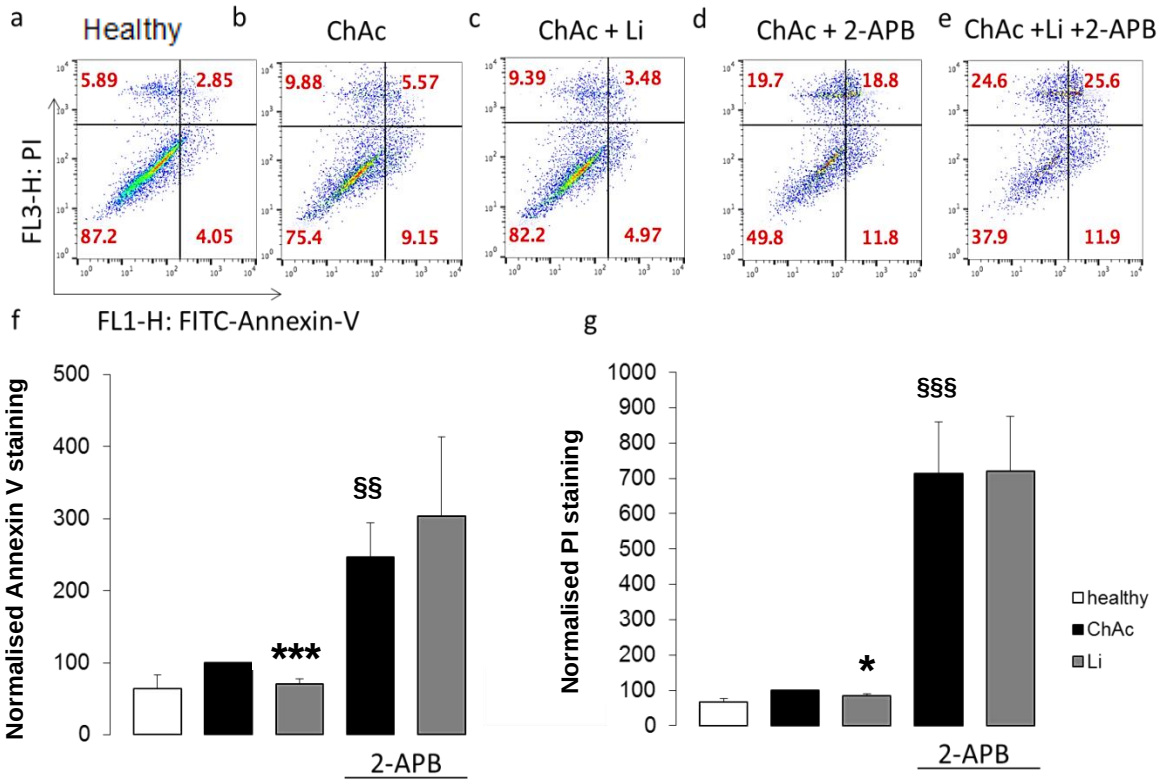

Figure 9: Effect of lithium on phosphatidylserine translocation and propidium iodide uptake in fibroblasts isolated from healthy donors and ChAc patients without and with Orai1 blocker 2-APB.

(a-e) Representative dot blots of propidium iodide staining versus annexin-V-binding fibroblasts isolated from healthy donors, untreated ChAc patients or treated with lithium (24 hours, 2mM) alone, or treated with Orai1 blocker 2-APB (24 hours, 50 µM) alone, or treated with both, lithium (2 mM) and 2-APB (50 µM) together for 24 hours. (f) Arithmetic means (±SEM, n=4-5 individuals) of percentage of annexin-V-binding fibroblasts isolated from healthy donors, or from ChAc patients untreated, or treated with lithium (24 hours, 2mM) alone, or treated with Orai1 blocker 2-APB (24 hours, 50 µM) alone, or treated with both, lithium (2 mM) and 2-APB (50 µM) together for 24 hours. All values were expressed in percent of the value in untreated fibroblasts isolated from ChAc patients. (g) Arithmetic means (±SEM, n=4-5 individuals) of the percentage of propidium iodide staining fibroblasts isolated from healthy donors, or from ChAc patients untreated, or treated with lithium (24 hours, 2mM) alone, or treated with Orai1 blocker 2-APB (24 hours, 50 µM) alone, or treated with both, lithium (2 mM) and 2-APB (50 µM) together for 24 hours. All values were

expressed in percent of the value in untreated fibroblasts isolated from ChAc patients. * p<0.05, *** p<0.001 indicates a statistically significant difference compared to the respective value in untreated ChAc fibroblasts. §§ p<0.01, §§§ p<0.001 indicates a statistically significant difference compared to the respective value in the absence of 2-APB. Figure adapted from (Pelzl et al., 2017a), changed.

4.6 Orai1 and STIM1 transcript and protein levels in neurons differentiated from ChAc patients

qRT-PCR was performed to quantify the mRNA expression of Orai1 and STIM1 in both healthy and ChAc iPSC-differentiated neurons, and the result showed that the transcript levels of Orai1 and STIM1 in ChAc neurons were significantly low compared with healthy neurons (Figure 10).

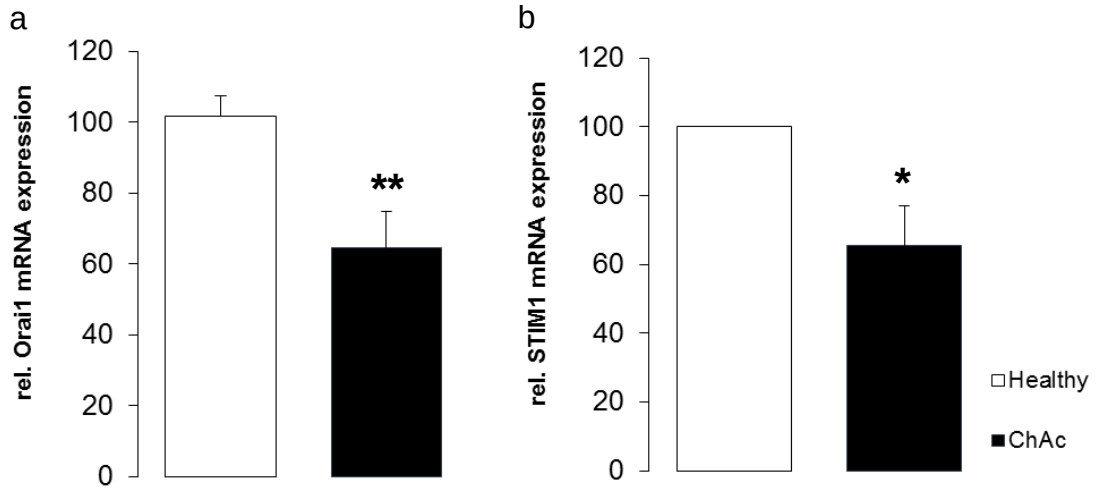

Figure 10: Orai1 and STIM1 transcript levels comparison between iPSCs-differentiated neurons from healthy donors and ChAc patients

Arithmetic means (±SEM, n=4) of (a) Orai1 and (b) STIM1 transcript levels in neurons isolated from healthy donors and ChAc patients. * p<0.05, ** p<0.01 indicates a statistically significant difference compared to the respective value in iPSC-differentiated neurons from healthy donors. Figure adapted from (Pelzl et al., 2017b), changed.

The difference in transcript levels reflected on protein abundance and made it in iPSC-differentiated neurons from ChAc patients significantly lower than those from healthy donors (Figure 11).

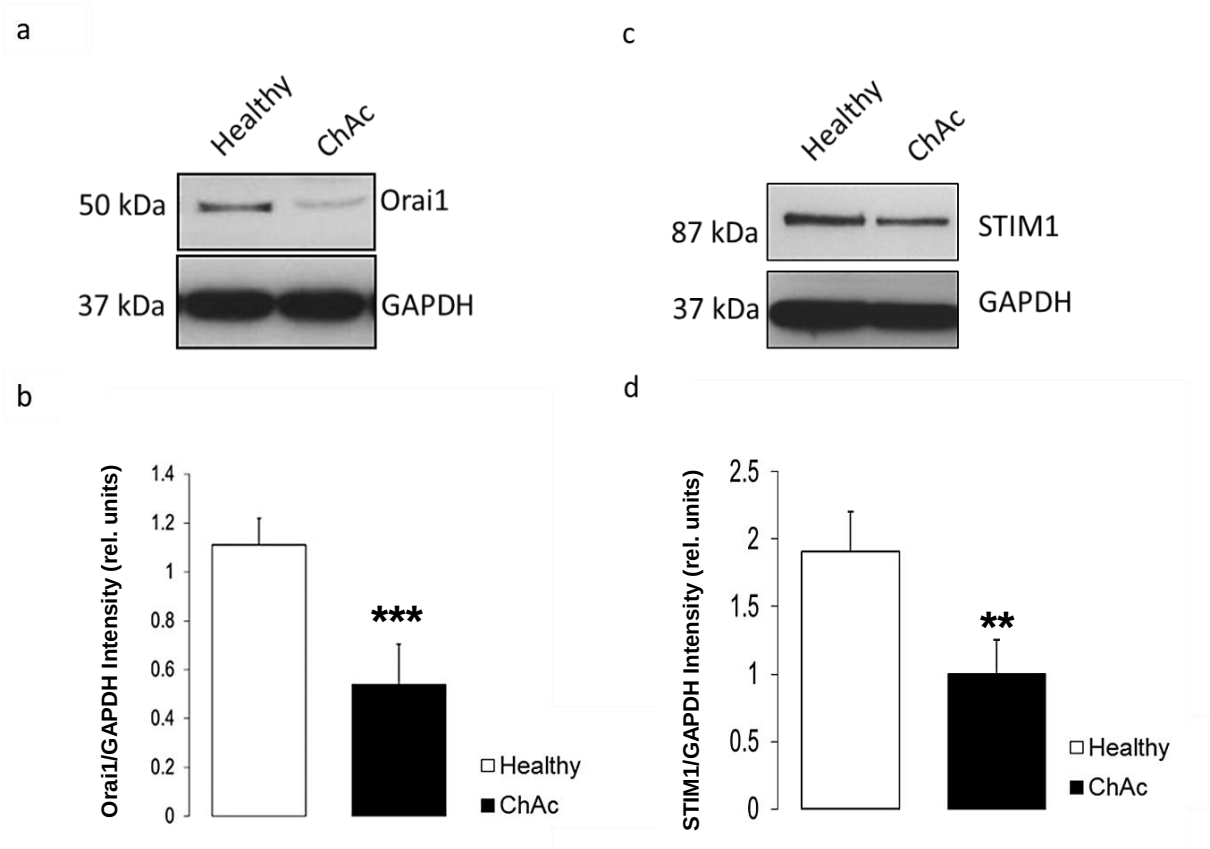

Figure 11: Orai1 and STIM1 protein abundance in iPSC-differentiated neurons from healthy donors and ChAc patients.

Original western blot of (a) Orai1 and (c) STIM1 protein abundance in iPSCs-differentiated neurons from healthy donors (Healthy) compared with neurons differentiated from ChAc patients (ChAc). (b) Arithmetic means (±SEM, n=4) of Orai1 protein levels in neurons isolated from healthy donors and ChAc patients. (d) Arithmetic means (±SEM, n=3) of STIM1 protein levels in neurons differentiated from healthy donors and ChAc patients.

** $p<0.01$, *** $p<0.001$ indicates a statistically significant difference compared to the respective value in iPSC-differentiated neurons from healthy donors. Figure adapted from (Pelzl et al., 2017b), changed.

4.7 Lithium treatment upregulates Orai1 and STIM1 mRNA expression and protein abundance in iPSC-differentiated ChAc neurons

To check the effect of lithium treatment on the transcript levels in iPSCs-differentiated ChAc neurons, neurons were treated with lithium (2 mM) for 24 hours and then qRT-PCR was applied (see 3.3). The results showed a significant increase in the transcript levels of Orai1 and STIM1 in lithium-treated neurons than untreated ones (Figure 12). To study the possible pathway of the effect that lithium does on the transcription of Orai1 and STIM1, the role of the serum & glucocorticoid-inducible kinase (SGK1) was checked as it regulates the transcription of Orai1 and STIM1 (Eylenstein et al., 2011). For this purpose, neurons were treated additionally with (10 µM) GSK650394, SGK1 inhibitor, which reversed the effect of lithium. The transcript levels of Orai1 and STIM1 were in neurons treated with lithium and GSK650394 together significantly lower than lithium just treated neurons, and even lower than untreated ChAc neurons (Figure 12).

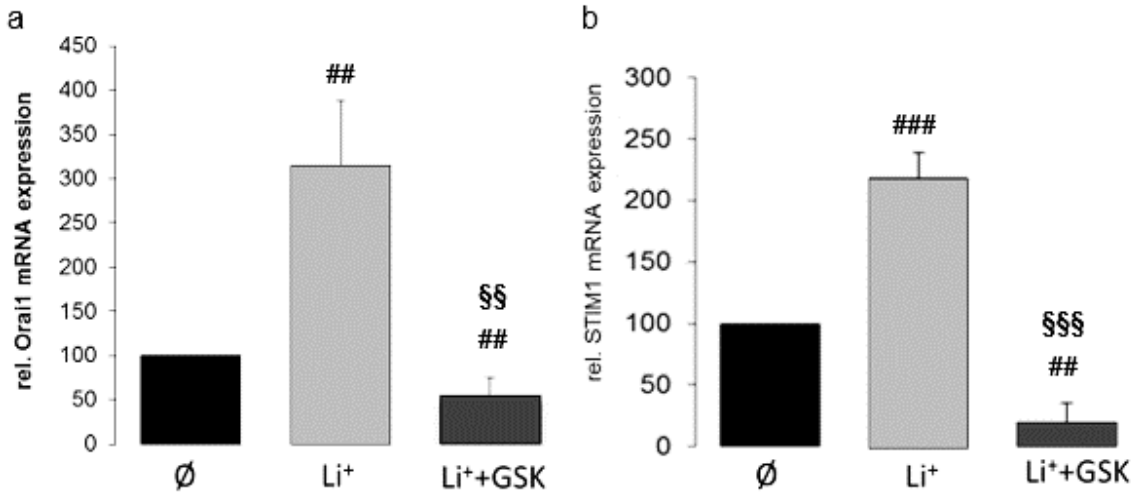

Figure 12: Transcription levels of Orai1 and STIM1 after lithium treatment with and without SGK1 inhibitor GSK650394 in iPSC-differentiated neurons from ChAc patients.

Arithmetic means of (a) Orai1 and (b) STIM1 mRNA abundance in untreated (Ø) iPSCs-differentiated ChAc neurons and after 24 h of lithium (2 mM) treatment without (Li^+) and with (Li^++GSK) presence of SGK1 inhibitor GSK650394 (10 µM). ## $p<0.01$, ### $p<0.001$ indicates statistically significant difference compared to untreated neurons. §§ $p<0.01$, §§§$p<0.001$ indicates a statistically significant difference compared to the respective value of lithium alone treated neurons. Figure adapted from (Pelzl et al., 2017b), changed.

Western blotting was used to check if the effect of lithium treatment was the same on protein abundance as mRNA abundance.

Again, neurons were treated with (2 mM) lithium for 24 hours and that resulted in a significant increase of Orai1 and STIM1 protein abundance (Figure 13). Additional treatment with (10 µM) of SGK1 inhibitor GSK650394 reversed the effect of lithium and decreased the levels of Orai1 and STIM1 protein abundance (Figure 13).

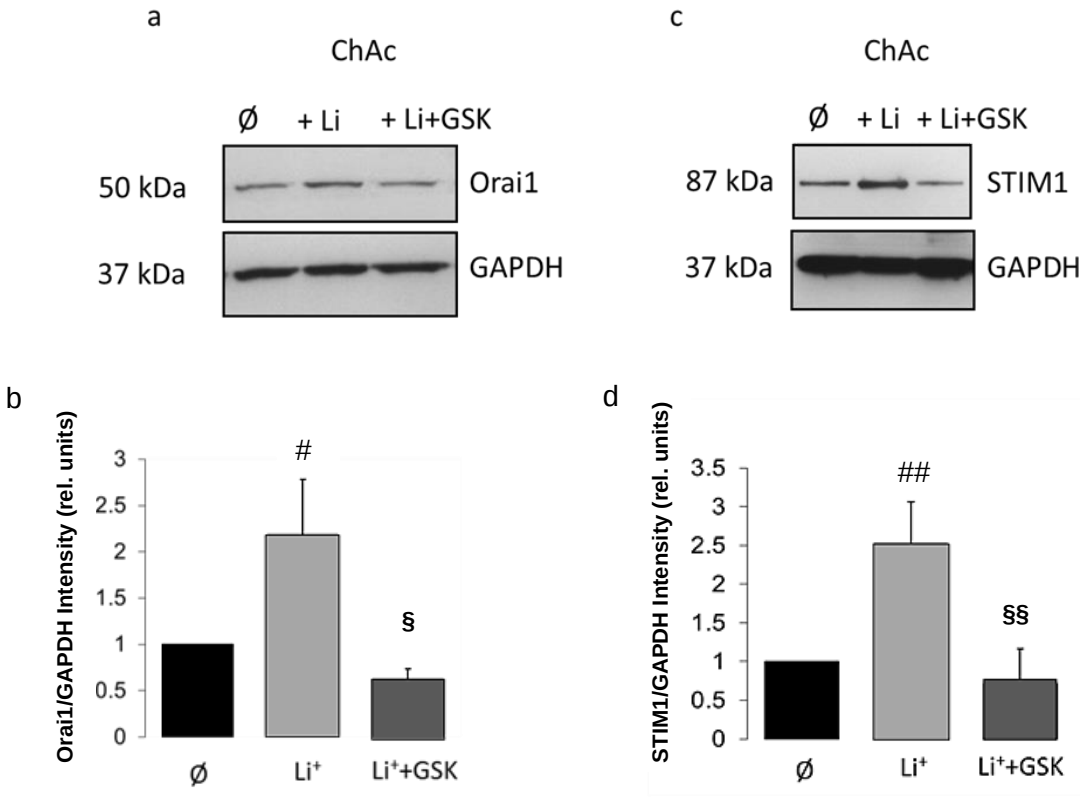

Figure 13: Protein abundance of Orai1 and STIM1 after lithium treatment without and with SGK1 inhibitor GSK650394 in iPSC-differentiated neurons from ChAc patients.

Original western blot of (a) Orai1 and (c) STIM1 protein abundance in untreated iPSCs-differentiated ChAc neurons (Ø) compared with neurons after (2 mM) lithium treatment for 24 hours without (+Li) and with (+Li+GSK) presence of (10 µM) SGK1 inhibitor GSK650394. (b) Arithmetic means (±SEM, n=4) of Orai1 protein levels in iPSCs-differentiated ChAc neurons without and with (2 mM) lithium treatment for 24 hours without or with addition of (10 µM) SGK1 inhibitor GSK650394.

(d) Arithmetic means (±SEM, n=3) of STIM1 protein levels in iPSCs-generated ChAc neurons without and with (2 mM) lithium treatment for 24 hours without or with addition of (10 µM) SGK1 inhibitor GSK650394. # $p<0.05$, ## $p<0.01$ indicates statistically significant to respective value in untreated samples. § $p<0.05$, §§ $p<0.01$ indicates statistically significant to respective value in lithium alone treatment. Figure adapted from (Pelzl et al., 2017b), changed.

4.8 Lithium treatment up-regulates SOCE in iPSC-differentiated ChAc neurons

To check if the decreased expression of Orai1 and STIM1 in ChAc generated neurons is paralleled by impairment of store-operated Ca^{2+} entry (SOCE), the calcium measurement method was processed using Fura2 fluorescence (see 3.5). Starting is cells exposure to the sarco-endoplasmic reticulum Ca^{2+}-ATPase (SERCA) inhibitor thapsigargin (1 µM) in the absence of extracellular Ca^{2+}, which empties the intracellular Ca^{2+} stores and causes an increase of $[Ca^{2+}]_i$ in healthy neurons similar to ChAc neurons (Figure 14 a-c). Then subsequent extracellular Ca^{2+} was added again in the presence of thapsigargin which caused a sharp increase of $[Ca^{2+}]_i$ referring to SOCE, and this effect was in ChAc neurons significantly less than healthy neurons, and this effect was significant in both the slope and the peak of $[Ca^{2+}]_i$ (Figure 14 a,d,e).

SOCE was measured also after treatment with (2 mM) lithium for 24 hours to check if this has an effect, and it resulted in a significant increase of both peak and slope of SOCE in lithium-treated samples in comparison to untreated ChAc neurons and resulted that SOCE in ChAc neurons treated with lithium was similar to untreated healthy neurons (Figure 14 d,e).

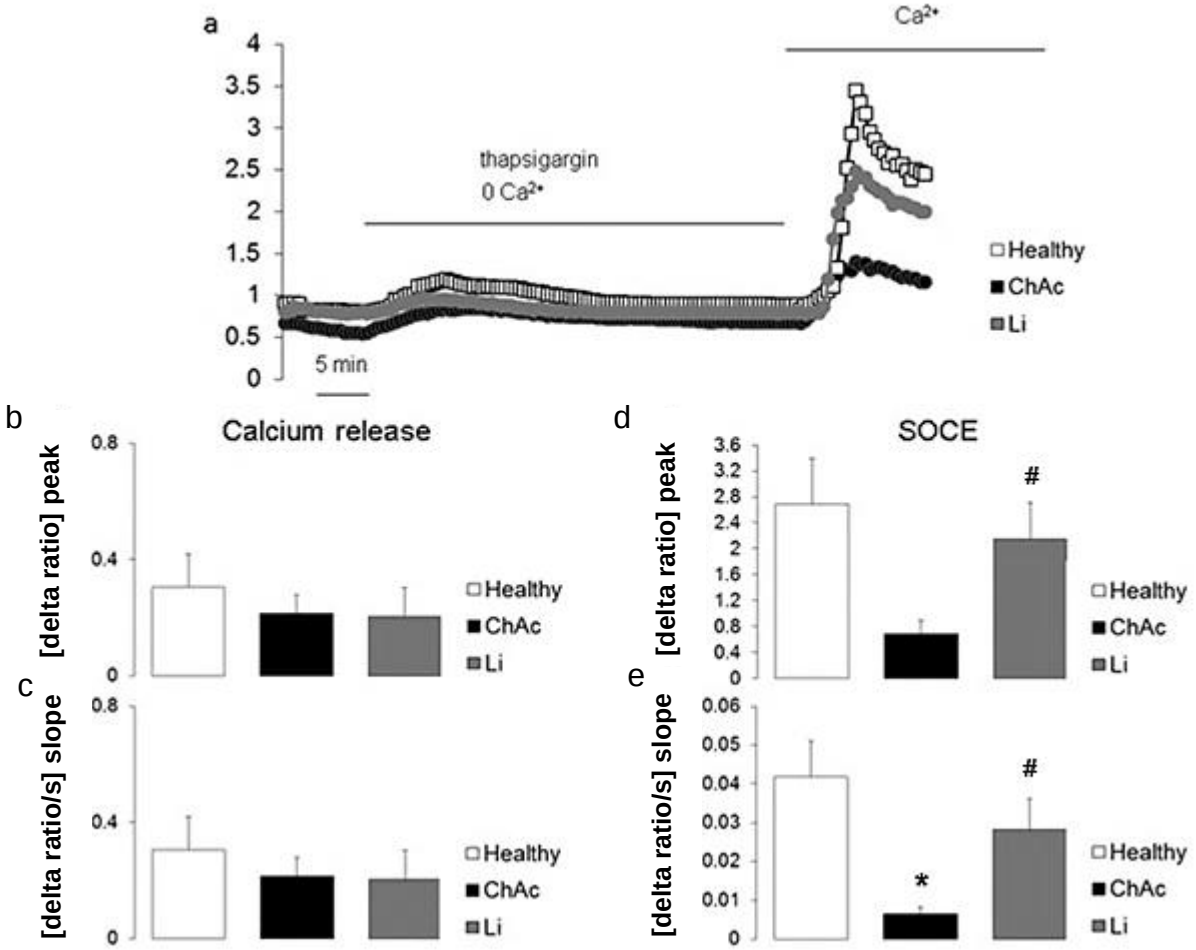

Figure 14: Effect of lithium treatment on intracellular Ca^{2+} release and SOCE in neurons differentiated from healthy donors and ChAc patients.

(a) Representative tracings of Fura-2 fluorescence-ratio in fluorescence spectrometry before and after extracellular Ca^{2+} removal (0 Ca^{2+}) and in the presence of thapsigargin (1 µM) and then re-addition of extracellular Ca^{2+} in iPSCs- differentiated neurons from healthy donors and from ChAc patients without and with (24 hours, 2 mM) lithium treatment. (b,c) Arithmetic means (±SEM, n=37-74 cells from 4 individuals) of peak (b) and slope (c) increase of Fura-2-fluorescence-ratio after addition of thapsigargin (1 µM) in iPSCs-differentiated neurons from healthy donors and in iPSCs- differentiated neurons from ChAc patients without and with lithium (24 hours, 2 mM) treatment. (d,e) Arithmetic means (±SEM, n=37-74 cells from 4 individuals) of peak (d) and slope (e) increase of Fura-2-fluorescence-ratio which follows the re-addition of extracellular Ca^{2+} in iPSC-generated neurons from healthy donors and in iPSCs-differentiated neurons from ChAc patients without and with lithium (24 hours, 2 mM) treatment. * $p<0.05$ indicates a statistically significant difference compared to respective value in neurons from healthy donors, # $p<0.05$ indicates a statistically significant difference compared to respective value in neurons from ChAc patients untreated with lithium. Figure adapted from (Pelzl et al., 2017b), changed.

4.9 Lithium supports the survival of ChAc iPSC-differentiated neurons

To check if the difference that was found in SOCE between healthy and ChAc neurons is paralleled with a difference in neuronal apoptosis, annexin-V binding and propidium iodide uptake were measured to identify the apoptotic neurons by flow cytometry (see 3.6). The results showed that the percentage of annexin-V-binding and propidium iodide uptake in iPSCs-differentiated neurons from ChAc patients was significantly higher than in iPSCs-differentiated neurons from healthy donors (Figure 15 a,b,f,g). Treatment with 2 µM lithium for 24 hours changed the results and showed that the percentage of annexin-V-binding and propidium iodide uptake in treated ChAc neurons was significantly lower than the percentage in untreated ChAc neurons (Figure 15 b,c,f,g). To check if the effect of lithium treatment on Orai1 has a further effect on apoptosis, ChAc neurons were treated with Orai1 blocker 2-APB (50 µM) with and without the addition of (2 mM) lithium. This exposure resulted in a significant increase in the percentage of annexin-V-binding and propidium iodide uptake and reversed the effect of lithium treatment on this percentage in ChAc neurons (Figure 15 d,e,f,g).

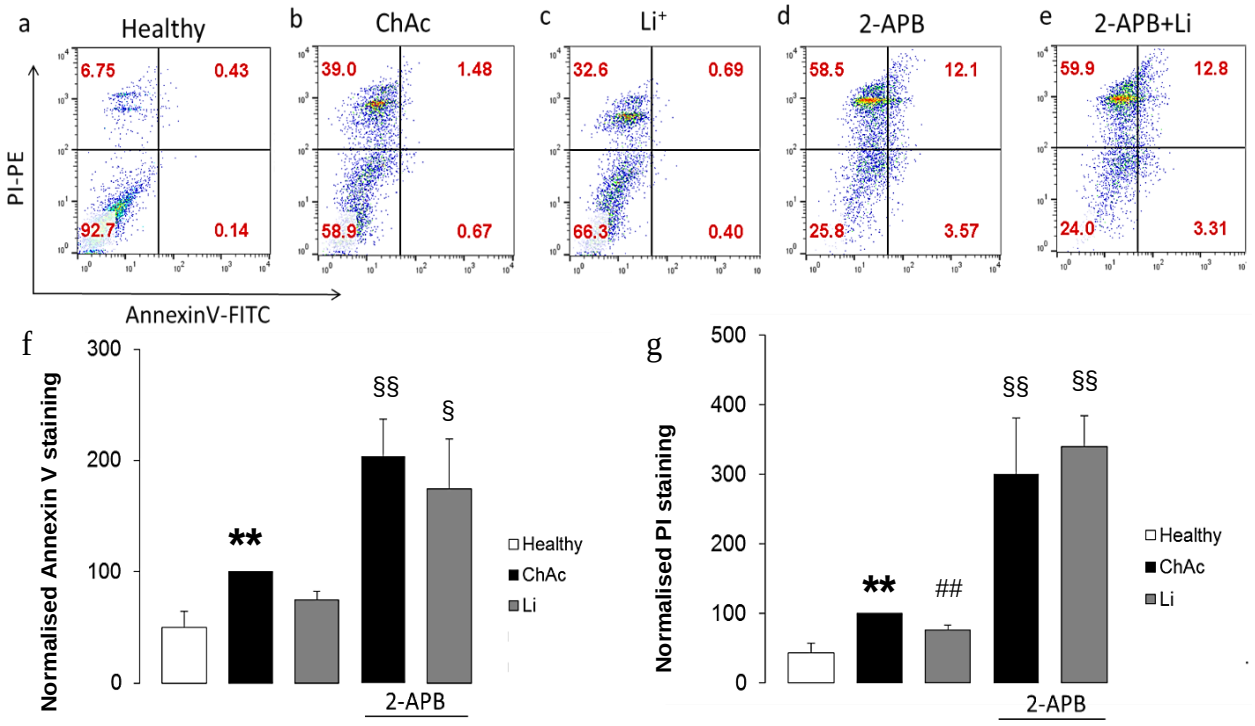

Figure 15: Effect of lithium and Orai1 blocking on phosphatidylserine translocation and propidium iodide uptake in iPSC-differentiated neurons from healthy donors and ChAc patients.

(a,e) Representative dot blots of annexin-V-binding versus propidium iodide staining in iPSCs-differentiated neurons from healthy donors and from ChAc patients without and with treatment with lithium (24 hours, 2 mM), and with 2-APB (50 µM) alone or with lithium treatment (2 mM) together. (f,g) Arithmetic means (±SEM, n=4-5 individuals) of normalized annexin-V-binding (f) or propidium iodide (g) stained iPSCs-differentiated neurons from healthy donors, ChAc patients without and with lithium (24 hours, 2 mM) treatment, with Orai1 blocker 2-APB (50 µM) alone or with lithium together. ** $p<0.01$ indicates a statistically significant difference compared to the respective value in neurons from healthy donors. ## $p<0.01$ indicates a statistically significant difference compared to the respective value in ChAc neurons without treatment. § $p<0.05$, §§ $p<0.01$ indicates a statistically significant difference compared to the respective value in ChAc neurons without 2-APB treatment. Figure adapted from (Pelzl et al., 2017b).

4.10 Inhibition of NFκB abrogates the effect of lithium on Orai1 and STIM1 mRNA and protein abundance in iPSC-differentiated ChAc neurons

To have a wider physiological insight of the pathway that makes lithium effective on the expression of Orai1 and STIM1, the role of NFκB, as a transcriptional activator of Orai1 and STIM1 (Eylenstein et al., 2012, Lang and Hoffmann, 2012), was checked. For this reason, iPSC-differentiated neurons from ChAc patients were treated with NFκB inhibitor wogonin. Wogonin is a known inhibitor of NFκB by inhibition of the phosphorylation of IκB and this prevents the translocation of NFκB into the nucleus (Zhao et al., 2010). To check if this is the effect also in ChAc neurons, we treated neurons with (50 µM) of NFκB inhibitor wogonin for 24 hours. Neurons were then treated with both lithium (2 mM) and wogonin (50 µM) for 24 hours. The results showed that wogonin alone treatment decreased significantly the transcript levels of Orai1 (Figure 16 a) and STIM1 (Figure 16 b). Treatment of neurons with lithium (24 hours, 2 mM) together with NFκB inhibitor wogonin (50 µM) resulted in abrogating the effect of lithium and a significant decrease in Orai1 and STIM1 transcript levels compared even with untreated ChAc neurons (Figure 16).

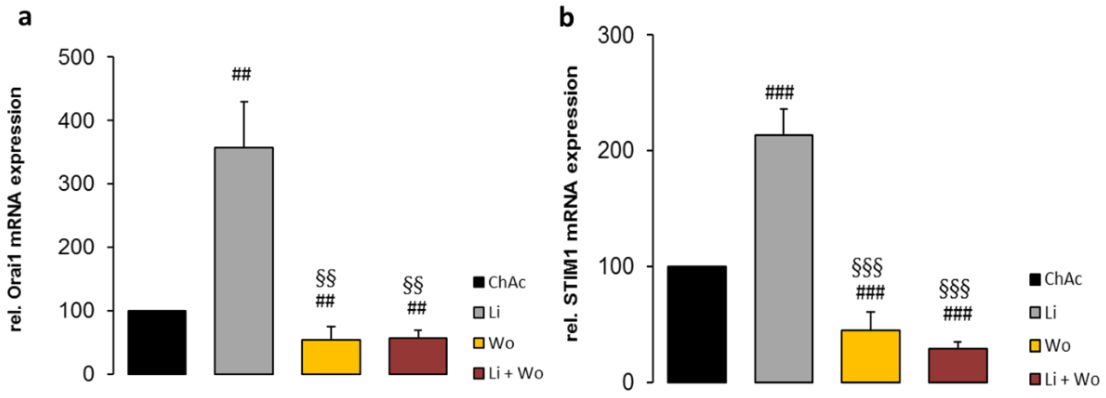

Figure 16: Effect of lithium treatment with and without NFκB inhibition by wogonin on Orai1 and STIM1 transcript levels in ChAc neurons.

Arithmetic means of (a) Orai1 and (b) STIM1 transcript levels in iPSCs-differentiated neurons from ChAc patients untreated, treated with lithium (24 hours, 2 mM) alone, treated with NFκB inhibitor wogonin (24 hours, 50 µM) alone or treatment with both lithium (2 mM) and wogonin (50 µM) for 24 hours. ## $p<0.01$, ### $p<0.001$ indicates statistically significant difference compared to respective value in untreated ChAc neurons. §§ $p<0.01$, §§§ $p<0.001$ indicates a statistically significant difference compared to the respective value in ChAc neurons treated with lithium alone. Figure adapted from (Sukkar et al., 2018), changed.

To check if the effect of NFκB inhibition with wogonin on the transcript levels of Orai1 and STIM1 is paralleled with the same effect on protein abundance, iPSC-differentiated neurons from ChAc patients were treated with lithium (2 mM) with and without wogonin (50 µM). Then western blotting was employed to check the protein abundance (see 3.4). The results showed that treatment with NFκB inhibitor wogonin (50 µM) together with lithium (2 mM), abrogated the effect of lithium and led to a significant decrease in the protein abundance Orai1 and STIM1 comparing to treatment with lithium (2 mM) alone (Figure 17).

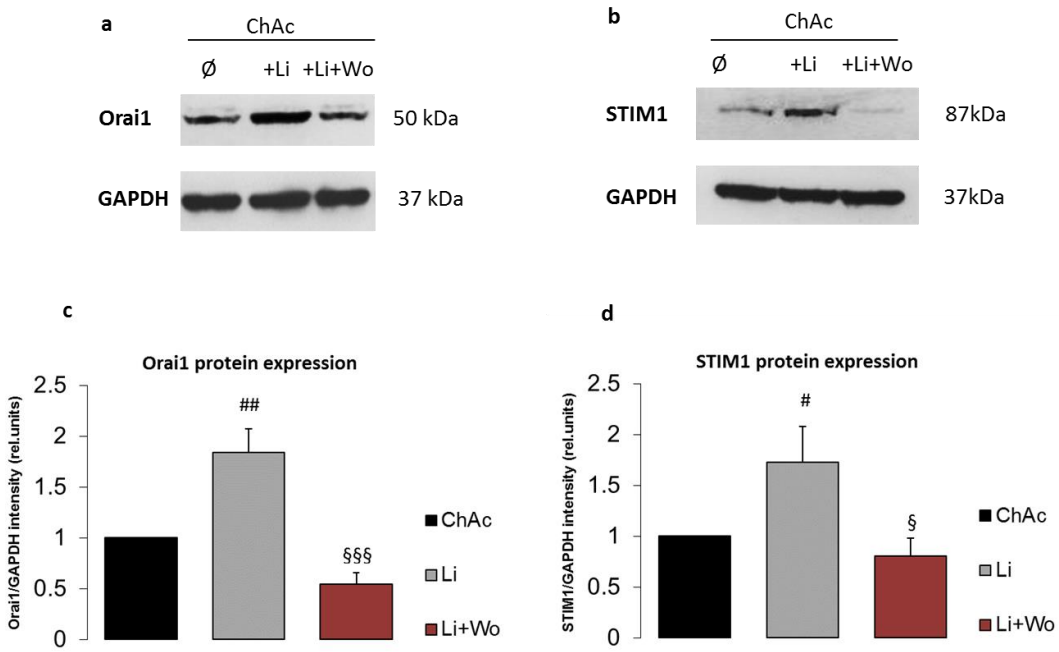

Figure 17: Influence of NFκB inhibitor wogonin on lithium treatment on the protein abundance of Orai1 and STIM1.

(a,b) Original western blot of Orai1 (a) and STIM1(b) protein abundance in iPSCs-differentiated ChAc neurons untreated or with lithium (24 hours,2 mM) treatment alone or together with NFκB inhibitor wogonin (50 µM). (c,d) Arithmetic means (±SEM, n=5) of Orai1 (c) and STIM1 (d) protein abundance in iPSCs-generated neurons from ChAc patients untreated, treated with lithium (24 hours, 2 mM) or treated with both lithium (2 mM) and NFκB inhibitor wogonin (50 µM) for 24 hours.

# $p<0.05$, ## $p<0.01$ indicates statistically significant difference compared to respective value in untreated ChAc neurons. § $p<0.05$, §§§ $p<0.001$ indicates a statistically significant difference compared to the respective value in ChAc neurons treated with lithium alone. Figure adapted from (Sukkar et al., 2018), changed.

4.11 Inhibition of NFκB abrogates the effect of lithium treatment on SOCE in iPSC-differentiated ChAc neurons

Fura-2 fluorescence was employed to check if the altered expression of Orai1 and STIM1 is also paralleled by changes in store-operated Ca^{2+} entry (SOCE) (see 3.5). After emptying the intracellular Ca^{2+} stores, a transient increase in $[Ca^{2+}]_i$ happened and this increase was in samples treated with lithium alone higher than those untreated ChAc neurons (Figure 18). Re-addition of extracellular Ca^{2+} in the presence of thapsigargin resulted in an increase of $[Ca^{2+}]_i$ significantly higher in samples treated with lithium (2mM) alone compared to untreated samples (Figure 18 d,e). SOCE was significantly decreased in ChAc neurons treated with NFκB inhibitor wogonin (50 μM) compared with untreated ChAc neurons and also with when lithium treatment was given with wogonin (Figure 18 d,e).

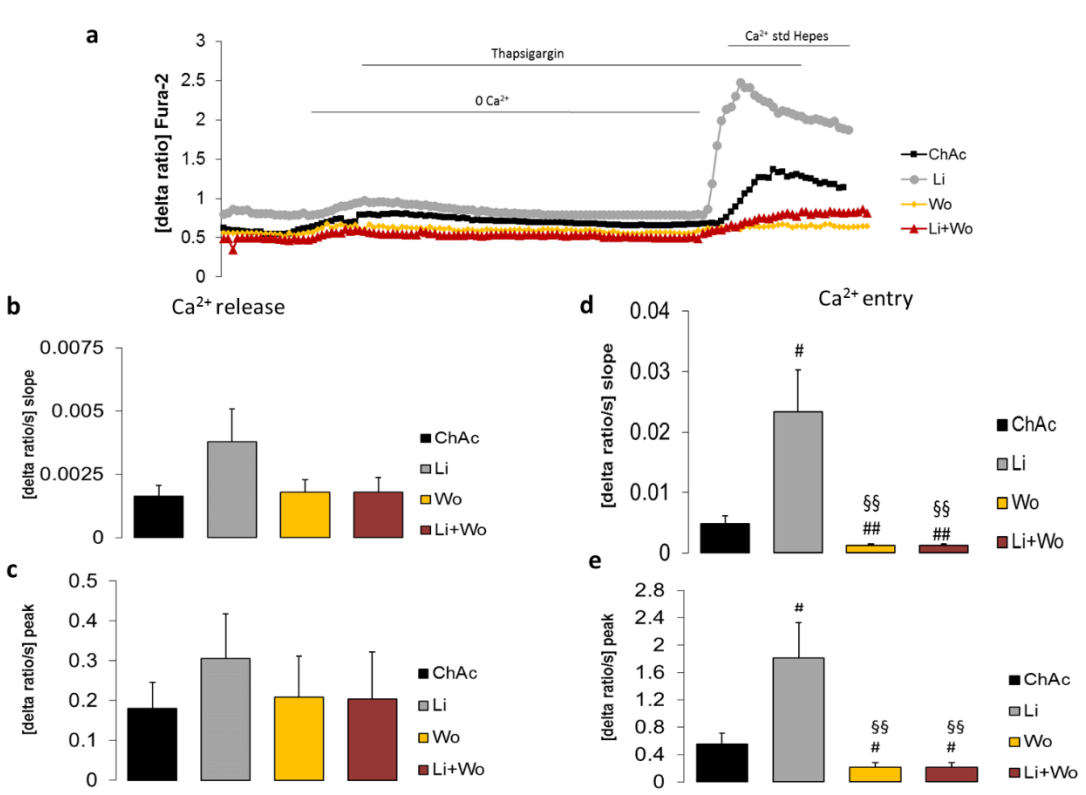

Figure 18: Intracellular Ca^{2+} release and store-operated Ca^{2+} entry (SOCE) after treatment with lithium without or with NFκB inhibitor wogonin in iPSC-differentiated neurons from ChAc patients.

(a) Representative tracings of Fura-2 fluorescence-ratio in fluorescence spectrometry before and following extracellular Ca^{2+} removal (0 Ca^{2+}) and then the addition of SERCA inhibitor thapsigargin (1 µM), followed by re-addition of extracellular Ca^{2+} in neurons generated from ChAc patients untreated and treated with lithium (24 hours, 2 mM) alone, with NFκB inhibitor wogonin (24 hours, 50 µM) alone, or both lithium and wogonin treatment. (b,c) Arithmetic means (±SEM, n=30-40 cells from 3 individuals) of (b) slope and (c) peak increase of Fura-2 fluorescence-ratio after the addition of (1 µM) thapsigargin in neurons generated from ChAc patients untreated and treated with lithium (24 hours, 2 mM) alone, with NFκB inhibitor wogonin (24 hours, 50 µM) alone, or both lithium and wogonin treatment. (d,e) Arithmetic means of (d) slope and (e) peak increase of Fura-2 fluorescence-ratio after re-addition of extracellular Ca^{2+} indicating SOCE in neurons generated from ChAc patients untreated and treated with lithium (24 hours, 2 mM) alone, with NFκB inhibitor wogonin (24 hours, 50 µM) alone, or both lithium and wogonin treatment. # $p<0.05$, ## $p<0.01$ indicates statistically significant difference compared to respective value in untreated ChAc neurons. §§ $p<0.01$ indicates a statistically significant difference to the respective value in ChAc neurons treated with lithium alone. Figure adapted from (Sukkar et al., 2018), changed.

4.12 Wogonin abrogates the effect of lithium on the survival of iPSC-differentiated neurons from ChAc patients

To explore if the inhibition of NFκB will influence the effect of lithium on the survival of ChAc neurons, again phosphatidylserine translocation utilizing annexin-V-binding and propidium iodide uptake was measured (see 3.6). The results showed that NFκB inhibitor wogonin treatment (50 µM) abrogated and reversed the effect of lithium when treated together and decreased both the annexin V binding percentage and propidium iodide uptake (Figure 21).

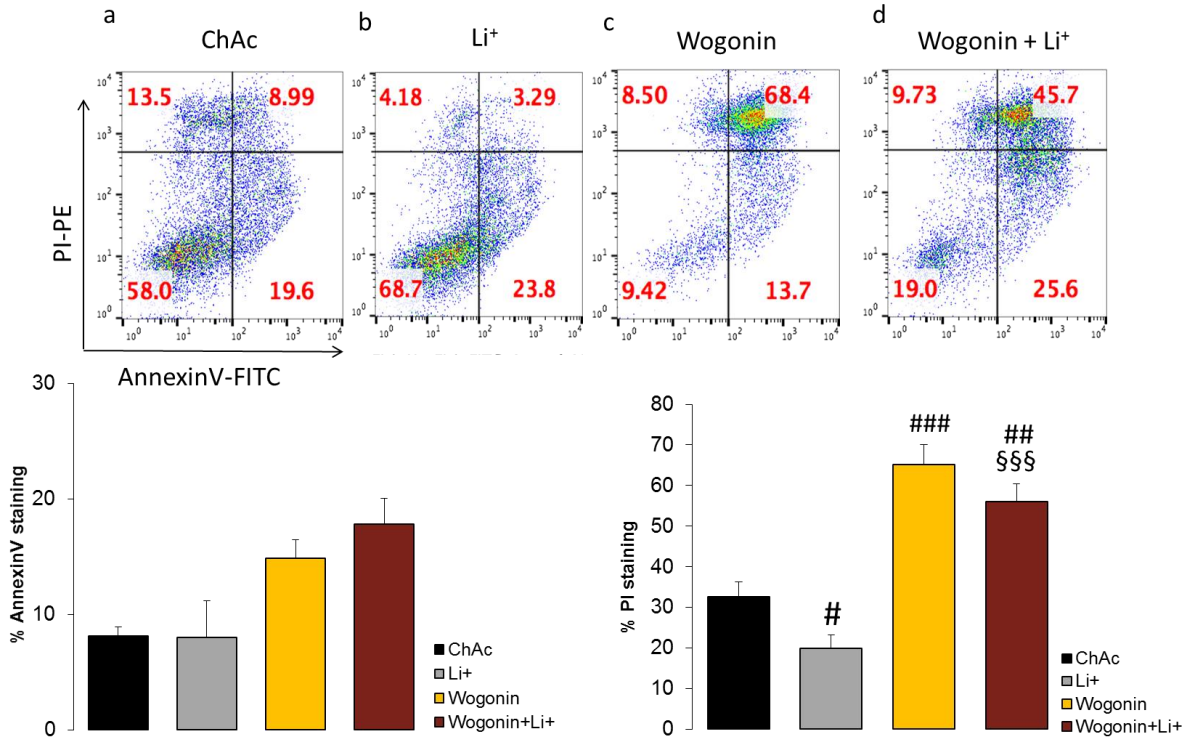

Figure 19: Influence of wogonin on the lithium effect on survival of iPSC-differentiated neurons from ChAc patients.

(a-d) Representative dot blots of annexin-V-binding versus propidium iodide staining in iPSCs-generated neurons from ChAc patients without and with treatment with lithium (24 hours, 2 mM), and with NFκB inhibitor wogonin (50 µM) alone or with lithium treatment (2 mM) together.

(e,f) Arithmetic means (±SEM, n=3 individuals) of normalized annexin-V-binding (e) or propidium iodide (f) stained iPSCs-generated neurons from ChAc patients without and with lithium (24 hours, 2 mM) treatment, with NFκB inhibitor wogonin (50 µM) alone or with lithium together. # $p<0.05$, ## $p<0.01$, ### $p<0.001$ indicates a statistically significant difference compared to the respective value in untreated ChAc neurons.

§§§ $p<0.001$ indicates a statistically significant difference compared to the respective value in neurons treated with lithium alone.

5. Discussion

This study is done to gain a pathophysiological insight into the effect of Chorea Acanthocytosis (ChAc), i.e. chorein deficiency, on cell survival and defective regulation of Orai1 and STIM1 expression with subsequent impairment of store-operated Ca^{2+} entry (SOCE). SOCE is responsible to trigger oscillations of cytosolic Ca^{2+} activity ($[Ca^{2+}]_i$) and thus affects cell survival and growth (Taylor et al., 2008, Heise et al., 2010, Parkash and Asotra, 2010). These oscillations appear when the increase of intracellular Ca^{2+} concentration occurs as repetitive short pulses, which has a role in the activation of Ca^{2+}-dependent transcription factors and the reorganization of actin filament network (Lang et al., 2006b, Lang and Stournaras, 2014), but when the increase of cytosolic Ca^{2+} activity is sustained, it leads to apoptosis in a variety of cell types (Green and Reed, 1998, Berridge et al., 2000, Lang and Hoffmann, 2012).

In this study, it is shown that SOCE was significantly down-regulated in fibroblasts and iPSC-differentiated neurons of ChAc patients compared with samples from healthy donors (Pelzl et al., 2017a, Pelzl et al., 2017b). The decrease of SOCE was synchronized by increased levels of apoptosis in ChAc fibroblasts and iPSC-differentiated neurons (Pelzl et al., 2017a, Pelzl et al., 2017b).

On the other hand, Orai isoforms and their regulators STIM 1 or 2 play a part in the Ca^{2+} oscillations and contribute to the survival and proliferation of tumor cells as well as neural stem/progenitor cells (Peinelt et al., 2006, Putney, 2007, Qu et al., 2011, Prevarskaya et al., 2011, Bergmeier et al., 2013, Prevarskaya et al., 2014, Somasundaram et al., 2014). The protein and mRNA abundance of Orai1 and STIM1 were significantly downregulated in ChAc iPSC-differentiated neurons compared to healthy donors (Pelzl et al., 2017b).

As ChAc disease has no clear cure so far (Velayos Baeza et al., 1993, Schneider et al., 2006), this study investigated the effect of the well-known psychiatric medicine, lithium, on the pathological variance in fibroblasts and iPSC-differentiated neurons of ChAc patients.

Lithium proved a protective effect in this study by reducing apoptosis and upregulating SOCE in fibroblasts and iPSC-differentiated neurons from ChAc patients (Pelzl et al., 2017a, Pelzl et al., 2017b).

The present study observes the signaling link between chorein deficiency and Orai1/STIM1. Accordingly, Orai1 and STIM1 transcript and protein levels were elevated by lithium treatment in ChAc, while the protective effect of lithium was abrogated by Orai1 inhibition

(Pelzl et al., 2017a, Pelzl et al., 2017b, Sukkar et al., 2018). These observations could speculate that lithium may modify the pathophysiology of neurodegeneration in partly by up-regulation of neuronal Orai1 and STIM1 expression as well as SOCE, which will lead to stimulate proliferation of neuronal progenitor cells and inhibit neuronal apoptosis (Somasundaram et al., 2014).

Previously was shown that Orai1 expression is regulated by the PI3K pathway (Raimondi and Falasca, 2011). This pathway includes activation of serum and glucocorticoid-inducible kinase (SGK1), which in turn phosphorylates the IKK complex and thus activates it (Lang et al., 2006a). The active IKK phosphorylates IκB proteins that are bounded to NFκB, and when the latter is free, it migrates into the nucleus causing the transcriptional activation of Orai1 and STIM1 and subsequently activating SOCE (Zhang et al., 2005a, Lang et al., 2012, Eylenstein et al., 2012) (Figure 20). Moreover, SGK1 is effective by the inhibition of Nedd4-2 induced degradation of Orai1 protein (Lang et al., 2012, Schmidt et al., 2014). Based on these observations, inhibition of SGK1 by GSK650394 in this study resulted in reversing the effect of lithium on SOCE and cell survival which highlights the impact of SGK1 on the protective role of lithium (Pelzl et al., 2017b).

The mechanisms that reflect the neuroprotective effect of lithium are several. It activates Akt which in turn phosphorylates BAD protein resulting in suppressing cell death (Chalecka-Franaszek and Chuang, 1999, Datta et al., 1997). Furthermore, lithium ions can also inhibit GSK-3 (Stambolic et al., 1996). This protective effect linking to many studies which showed that overexpression of GSK3-β caused apoptosis of neuronal PC12 cells (Pap and Cooper, 1998), and GSK3, showed to elevate apoptosis of neuronal SH-SY5Y cells (Bijur et al., 1999). In another study, cell death of sympathetic neurons that was mediated by loss of PI3K signaling was reduced by inhibition of GSK3 (Crowder and Freeman, 1998). These observations support the idea that GSK3 has a pro-apoptotic role in neuronal cells, and inhibition of GSK3 in these cells, which lithium does, improves the pro-survival PI3K signaling pathway (Maurer et al., 2014, Cross et al., 1995).

Along these lines, NFκB could be also activated in two ways; either by Akt activation or by partial inactivation of GSK-3: on the one hand, when Akt is active, it leads to IKK stimulation which in turn phosphorylates the IκB protein and p65/RelA subunit to end with enhanced activation of NFκB (Bai et al., 2009). On the other hand, GSK3 can phosphorylate the NFκB inhibitory protein NFκB2/ p100 and thus prevents its IκB-like role in

suppressing NFκB, which enables NFκB to complete its pro-survival and transcriptional role (Siebenlist et al., 1994, Ghosh and Karin, 2002, Busino et al., 2012, Fukushima et al., 2012).
Depending on these important observations, and as lithium is able to activate Akt and inhibit GSK3 as well, this could mean that the effect of lithium on the expression of Orai1 and STIM1 showed in this study, might be achieved through NFκB activation (Stambolic et al., 1996, Chalecka-Franaszek and Chuang, 1999).
As for experimental evidence, inhibition of NFκB by wogonin in this study decreased significantly Orai1 and STIM1 transcript levels as well as SOCE and induced apoptosis in fibroblasts and iPSC-differentiated neurons of ChAc patients (Sukkar et al., 2018). Moreover, it abrogated the stimulating effect of lithium, which reflects the stimulating effect of NFκB in neurons in both, the presence and absence of lithium, and highlights the potential role that NFκB may play in the effect of lithium (Sukkar et al., 2018). However, these observations are not evidencing whether NFκB has an inhibitory effect on neurodegeneration or not which is still to be investigated.
This study does not address the signaling linking for cell apoptosis. It is more probable that this signaling will contain a role of the PI3K pathway, which includes the kinase SGK1 (Raimondi and Falasca, 2011) and which are known for the upregulation of Orai1 (Lang et al., 2012). In view of the present study, the pathological suicidal death of neurons in ChAc patients, which is the decisive pathophysiological mechanism that leads to this devastating disease (Jung et al., 2011), could be delayed or even held by lithium treatment.
A good and also critical feature of lithium ions is their water-solubility and the ability to distribute throughout all of the body water in the same way as sodium ions (Na^+) (Sproule et al., 2000). Lithium can cross the blood-brain barrier (BBB) (Platman and Fieve, 1968). However, there are age-related changes in BBB as it becomes weaker by age which alters the uptake of lithium into the brain and thus affects the pharmacokinetics of lithium in the older adults (Mooradian, 1994, Sproule et al., 2000). Furthermore, the volume of distribution and renal clearance decreases with age also, and this emphasizes reducing the dose of lithium for older individuals (Hewick et al., 1977). Anyway, the onset age average of Chorea Acanthocytosis is 35 years old, which is early for the complications of lithium (Zhang et al., 2013). Studies showed neurotoxicity of lithium including prolonged recovery from lithium-induced delirium and adverse consequences on memory and speed of cognitive and psychomotor execution, but anyway, like the complications of weak BBB, these cases were

concerned in older individuals more compared with younger patients with bipolar disorder (Nambudiri et al., 1991, Pachet and Wisniewski, 2003, Zhang et al., 2013).

Limitations of the study include the sensitivity of iPSC-differentiated neurons as they were transferred from the institute where they were generated to the further experiments institute, and they many times were not usable when they arrived, as well the lack number of patients with ChAc.

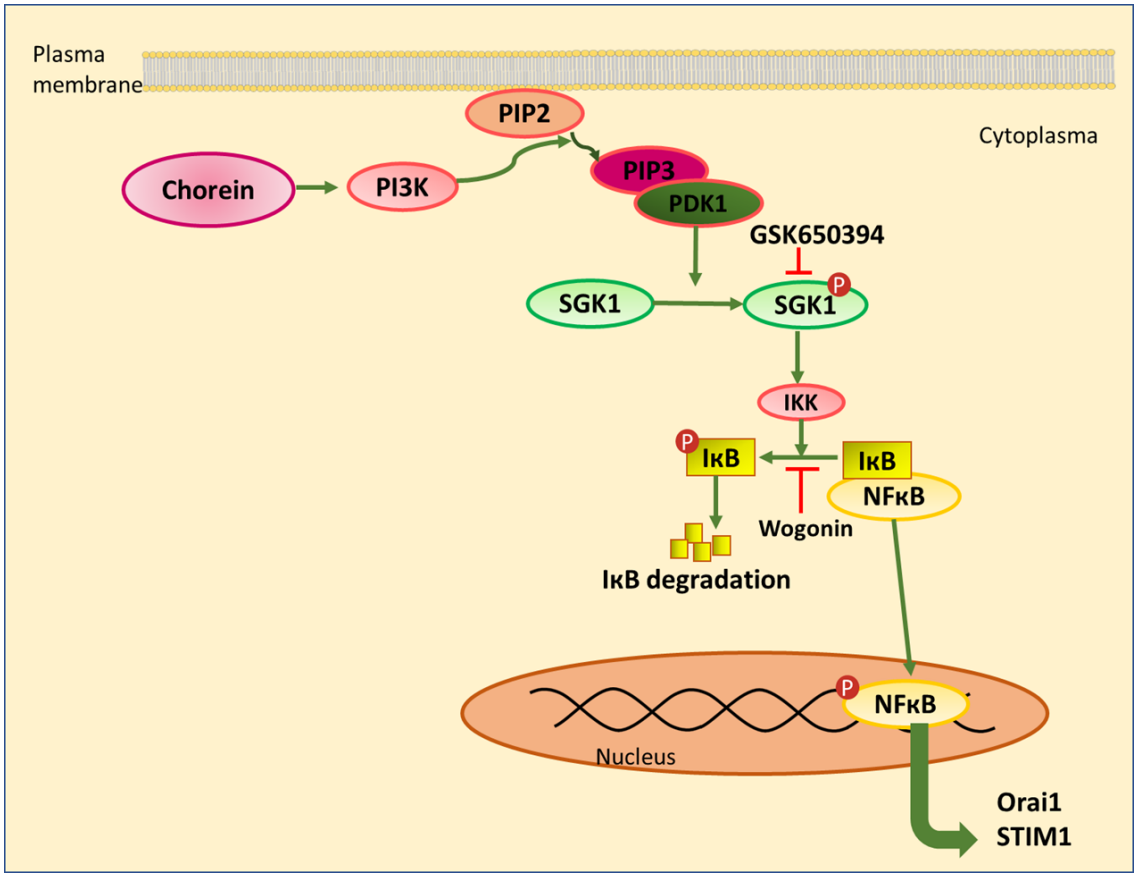

Figure 20: Postulated regulation of PI3K pathway via chorein.

Chorein interacts with PI3K and stimulates it (Wu et al., 2007, Foller et al., 2012, Honisch et al., 2015c). Activation of PI3K leads to the formation of phosphatidylinositol 3,4,5-triphosphate (PIP3) from phosphatidylinositol 4,5-bisphosphate (PIP2) (Scharenberg and Kinet, 1998).

3-phosphoinositide-dependent kinase (PDK1), which binds to PIP3, leads to phosphorylation and thus the activation of SGK1 (Lang and Cohen, 2001). In turn, SGK1 leads to phosphorylation of IκB and the translocation of NFκB into the nucleus where it works on the upregulation of Orai1 and STIM1 (Lang et al., 2006a, Eylenstein et al., 2012). Accordingly, when chorein is nonfunctional, i.e. Chorea Acanthocytosis, this pathway will be inactive which leads to downregulation of Orai1 and STIM1 and thus SOCE, as well increases apoptosis levels (Velayos Baeza et al., 1993, Pelzl et al., 2017a, Pelzl et al., 2017b, Sukkar et al., 2018, Foller et al., 2012, Honisch et al., 2015c).

6. Conclusion

The present observations reveal that Chorea Acanthocytosis leads to the downregulation of Orai1 and STIM1 expressions, as well as store-operated Ca^{2+} entry which leads to compromising neuronal cell survival. On the contrary, lithium up-regulates store-operated Ca^{2+} entry and reduces neuronal apoptosis, beneficial effects abrogated by the pharmaceutical inhibitions of Orai1 or its regulators SGK1 and NFκB.

7. References

ALDA, M. 2015. Lithium in the treatment of bipolar disorder: pharmacology and pharmacogenetics. *Mol Psychiatry,* 20**,** 661-70.

ALESUTAN, I., SEIFERT, J., PAKLADOK, T., RHEINLAENDER, J., LEBEDEVA, A., TOWHID, S. T., STOURNARAS, C., VOELKL, J., SCHAFFER, T. E. & LANG, F. 2013. Chorein sensitivity of actin polymerization, cell shape and mechanical stiffness of vascular endothelial cells. *Cell Physiol Biochem,* 32**,** 728-42.

ALVAREZ, G., MUNOZ-MONTANO, J. R., SATRUSTEGUI, J., AVILA, J., BOGONEZ, E. & DIAZ-NIDO, J. 2002. Regulation of tau phosphorylation and protection against beta-amyloid-induced neurodegeneration by lithium. Possible implications for Alzheimer's disease. *Bipolar Disord,* 4**,** 153-65.

AVILA, J., LEON-ESPINOSA, G., GARCIA, E., GARCIA-ESCUDERO, V., HERNANDEZ, F. & DEFELIPE, J. 2012. Tau Phosphorylation by GSK3 in Different Conditions. *Int J Alzheimers Dis,* 2012**,** 578373.

BADER, B., WALKER, R. H., VOGEL, M., PROSIEGEL, M., MCINTOSH, J. & DANEK, A. 2010. Tongue protrusion and feeding dystonia: a hallmark of chorea-acanthocytosis. *Mov Disord,* 25**,** 127-9.

BAI, D., UENO, L. & VOGT, P. K. 2009. Akt-mediated regulation of NFkappaB and the essentialness of NFkappaB for the oncogenicity of PI3K and Akt. *Int J Cancer,* 125**,** 2863-70.

BASU, A. & HALDAR, S. 1998. The relationship between Bcl2, Bax and p53: consequences for cell cycle progression and cell death. *Mol Hum Reprod,* 4**,** 1099-109.

BAUER, M., ALDA, M., PRILLER, J., YOUNG, L. T. & INTERNATIONAL GROUP FOR THE STUDY OF LITHIUM TREATED, P. 2003. Implications of the neuroprotective effects of lithium for the treatment of bipolar and neurodegenerative disorders. *Pharmacopsychiatry,* 36 Suppl 3**,** S250-4.

BEAULIEU, J. M., SOTNIKOVA, T. D., YAO, W. D., KOCKERITZ, L., WOODGETT, J. R., GAINETDINOV, R. R. & CARON, M. G. 2004. Lithium antagonizes dopamine-dependent behaviors mediated by an AKT/glycogen synthase kinase 3 signaling cascade. *Proc Natl Acad Sci U S A,* 101**,** 5099-104.

BERGMEIER, W., WEIDINGER, C., ZEE, I. & FESKE, S. 2013. Emerging roles of store-operated Ca(2)(+) entry through STIM and ORAI proteins in immunity, hemostasis and cancer. *Channels (Austin),* 7**,** 379-91.

BERRIDGE, M. J. 1993. Inositol trisphosphate and calcium signalling. *Nature,* 361**,** 315-25.

BERRIDGE, M. J., BOOTMAN, M. D. & RODERICK, H. L. 2003. Calcium signalling: dynamics, homeostasis and remodelling. *Nat Rev Mol Cell Biol,* 4**,** 517-29.

BERRIDGE, M. J., LIPP, P. & BOOTMAN, M. D. 2000. The versatility and universality of calcium signalling. *Nat Rev Mol Cell Biol,* 1**,** 11-21.

BIJUR, G. N., DAVIS, R. E. & JOPE, R. S. 1999. Rapid activation of heat shock factor-1 DNA binding by H2O2 and modulation by glutathione in human neuroblastoma and Alzheimer's disease cybrid cells. *Brain Res Mol Brain Res,* 71**,** 69-77.

BIRD, G. S., DEHAVEN, W. I., SMYTH, J. T. & PUTNEY, J. W., JR. 2008. Methods for studying store-operated calcium entry. *Methods,* 46**,** 204-12.

BOOTMAN, M. D., BERRIDGE, M. J. & RODERICK, H. L. 2002. Calcium signalling: more messengers, more channels, more complexity. *Curr Biol,* 12**,** R563-5.
BURGOYNE, R. D. 2007. Neuronal calcium sensor proteins: generating diversity in neuronal Ca2+ signalling. *Nat Rev Neurosci,* 8**,** 182-93.
BUSINO, L., MILLMAN, S. E., SCOTTO, L., KYRATSOUS, C. A., BASRUR, V., O'CONNOR, O., HOFFMANN, A., ELENITOBA-JOHNSON, K. S. & PAGANO, M. 2012. Fbxw7alpha- and GSK3-mediated degradation of p100 is a pro-survival mechanism in multiple myeloma. *Nat Cell Biol,* 14**,** 375-85.
CADE, J. F. 1949. Lithium salts in the treatment of psychotic excitement. *Med J Aust,* 2**,** 349-52.
CARAFOLI, E. 2002. Calcium signaling: a tale for all seasons. *Proc Natl Acad Sci U S A,* 99**,** 1115-22.
CHALECKA-FRANASZEK, E. & CHUANG, D. M. 1999. Lithium activates the serine/threonine kinase Akt-1 and suppresses glutamate-induced inhibition of Akt-1 activity in neurons. *Proc Natl Acad Sci U S A,* 96**,** 8745-50.
CLAPHAM, D. E. 1995. Calcium signaling. *Cell,* 80**,** 259-68.
CROSS, D. A., ALESSI, D. R., COHEN, P., ANDJELKOVICH, M. & HEMMINGS, B. A. 1995. Inhibition of glycogen synthase kinase-3 by insulin mediated by protein kinase B. *Nature,* 378**,** 785-9.
CROSSLEY, N. A. & BAUER, M. 2007. Acceleration and augmentation of antidepressants with lithium for depressive disorders: two meta-analyses of randomized, placebo-controlled trials. *J Clin Psychiatry,* 68**,** 935-40.
CROWDER, R. J. & FREEMAN, R. S. 1998. Phosphatidylinositol 3-kinase and Akt protein kinase are necessary and sufficient for the survival of nerve growth factor-dependent sympathetic neurons. *J Neurosci,* 18**,** 2933-43.
DARZYNKIEWICZ, Z., JUAN, G., LI, X., GORCZYCA, W., MURAKAMI, T. & TRAGANOS, F. 1997. Cytometry in cell necrobiology: analysis of apoptosis and accidental cell death (necrosis). *Cytometry,* 27**,** 1-20.
DATTA, S. R., DUDEK, H., TAO, X., MASTERS, S., FU, H., GOTOH, Y. & GREENBERG, M. E. 1997. Akt phosphorylation of BAD couples survival signals to the cell-intrinsic death machinery. *Cell,* 91**,** 231-41.
DE VASCONCELLOS, A. P., NIETO, F. B., CREMA, L. M., DIEHL, L. A., DE ALMEIDA, L. M., PREDIGER, M. E., DA ROCHA, E. R. & DALMAZ, C. 2006. Chronic lithium treatment has antioxidant properties but does not prevent oxidative damage induced by chronic variate stress. *Neurochem Res,* 31**,** 1141-51.
DOBSON-STONE, C., VELAYOS-BAEZA, A., FILIPPONE, L. A., WESTBURY, S., STORCH, A., ERDMANN, T., WROE, S. J., LEENDERS, K. L., LANG, A. E., DOTTI, M. T., FEDERICO, A., MOHIDDIN, S. A., FANANAPAZIR, L., DANIELS, G., DANEK, A. & MONACO, A. P. 2004. Chorein detection for the diagnosis of chorea-acanthocytosis. *Ann Neurol,* 56**,** 299-302.
ELMORE, S. 2007. Apoptosis: a review of programmed cell death. *Toxicol Pathol,* 35**,** 495-516.
EUROPEAN MOLECULAR BIOLOGY LABORATORY. 2011. Available: https://www.ebi.ac.uk/intact/interaction/EBI-1969677 [Accessed].
EYLENSTEIN, A., GEHRING, E. M., HEISE, N., SHUMILINA, E., SCHMIDT, S., SZTEYN, K., MUNZER, P., NURBAEVA, M. K., EICHENMULLER, M., TYAN, L., REGEL, I., FOLLER, M., KUHL, D., SOBOLOFF, J., PENNER, R. &

LANG, F. 2011. Stimulation of Ca2+-channel Orai1/STIM1 by serum- and glucocorticoid-inducible kinase 1 (SGK1). *FASEB J,* 25**,** 2012-21.
EYLENSTEIN, A., SCHMIDT, S., GU, S., YANG, W., SCHMID, E., SCHMIDT, E. M., ALESUTAN, I., SZTEYN, K., REGEL, I., SHUMILINA, E. & LANG, F. 2012. Transcription factor NF-kappaB regulates expression of pore-forming Ca2+ channel unit, Orai1, and its activator, STIM1, to control Ca2+ entry and affect cellular functions. *J Biol Chem,* 287**,** 2719-30.
FESKE, S., GWACK, Y., PRAKRIYA, M., SRIKANTH, S., PUPPEL, S. H., TANASA, B., HOGAN, P. G., LEWIS, R. S., DALY, M. & RAO, A. 2006. A mutation in Orai1 causes immune deficiency by abrogating CRAC channel function. *Nature,* 441**,** 179-85.
FESKE, S., SKOLNIK, E. Y. & PRAKRIYA, M. 2012. Ion channels and transporters in lymphocyte function and immunity. *Nat Rev Immunol,* 12**,** 532-47.
FOLLER, M., HERMANN, A., GU, S., ALESUTAN, I., QADRI, S. M., BORST, O., SCHMIDT, E. M., SCHIELE, F., VOM HAGEN, J. M., SAFT, C., SCHOLS, L., LERCHE, H., STOURNARAS, C., STORCH, A. & LANG, F. 2012. Chorein-sensitive polymerization of cortical actin and suicidal cell death in chorea-acanthocytosis. *FASEB J,* 26**,** 1526-34.
FUKUSHIMA, H., MATSUMOTO, A., INUZUKA, H., ZHAI, B., LAU, A. W., WAN, L., GAO, D., SHAIK, S., YUAN, M., GYGI, S. P., JIMI, E., ASARA, J. M., NAKAYAMA, K., NAKAYAMA, K. I. & WEI, W. 2012. SCF(Fbw7) modulates the NFkB signaling pathway by targeting NFkB2 for ubiquitination and destruction. *Cell Rep,* 1**,** 434-43.
GAO, Y., LEI, Z., LU, C., ROISEN, F. J. & EL-MALLAKH, R. S. 2010. Effect of ionic stress on apoptosis and the expression of TRPM2 in human olfactory neuroepithelial-derived progenitors. *World J Biol Psychiatry,* 11**,** 972-84.
GHOSH, S. & KARIN, M. 2002. Missing pieces in the NF-kappaB puzzle. *Cell,* 109 Suppl**,** S81-96.
GREEN, D. R. & REED, J. C. 1998. Mitochondria and apoptosis. *Science,* 281**,** 1309-12.
GWACK, Y., SRIKANTH, S., FESKE, S., CRUZ-GUILLOTY, F., OH-HORA, M., NEEMS, D. S., HOGAN, P. G. & RAO, A. 2007. Biochemical and functional characterization of Orai proteins. *J Biol Chem,* 282**,** 16232-43.
HAUSER, S., HOFLINGER, P., THEURER, Y., RATTAY, T. W. & SCHOLS, L. 2016. Generation of induced pluripotent stem cells (iPSCs) from a hereditary spastic paraplegia patient carrying a homozygous Y275X mutation in CYP7B1 (SPG5). *Stem Cell Res,* 17**,** 437-440.
HAYASHI, T., KISHIDA, M., NISHIZAWA, Y., IIJIMA, M., KORIYAMA, C., NAKAMURA, M., SANO, A. & KISHIDA, S. 2012. Subcellular localization and putative role of VPS13A/chorein in dopaminergic neuronal cells. *Biochem Biophys Res Commun,* 419**,** 511-6.
HEISE, N., PALME, D., MISOVIC, M., KOKA, S., RUDNER, J., LANG, F., SALIH, H. R., HUBER, S. M. & HENKE, G. 2010. Non-selective cation channel-mediated Ca2+-entry and activation of Ca2+/calmodulin-dependent kinase II contribute to G2/M cell cycle arrest and survival of irradiated leukemia cells. *Cell Physiol Biochem,* 26**,** 597-608.
HEWICK, D. S., NEWBURY, P., HOPWOOD, S., NAYLOR, G. & MOODY, J. 1977. Age as a factor affecting lithium therapy. *Br J Clin Pharmacol,* 4**,** 201-5.

HOGAN, P. G., LEWIS, R. S. & RAO, A. 2010. Molecular basis of calcium signaling in lymphocytes: STIM and ORAI. *Annu Rev Immunol,* 28**,** 491-533.
HONISCH, S., FEHRENBACHER, B., LEBEDEVA, A., ALESUTAN, I., CASTOR, T., ALKAHTANI, S., ALARIFI, S., SCHALLER, M., STOURNARAS, C. & LANG, F. 2015a. Chorein Sensitive Dopamine Release from Pheochromocytoma (PC12) Cells. *Neurosignals,* 23**,** 1-10.
HONISCH, S., GU, S., VOM HAGEN, J. M., ALKAHTANI, S., AL KAHTANE, A. A., TSAPARA, A., HERMANN, A., STORCH, A., SCHOLS, L., LANG, F. & STOURNARAS, C. 2015b. Chorein Sensitive Arrangement of Cytoskeletal Architecture. *Cell Physiol Biochem,* 37**,** 399-408.
HONISCH, S., YU, W., LIU, G., ALESUTAN, I., TOWHID, S. T., TSAPARA, A., SCHLEICHER, S., HANDGRETINGER, R., STOURNARAS, C. & LANG, F. 2015c. Chorein addiction in VPS13A overexpressing rhabdomyosarcoma cells. *Oncotarget,* 6**,** 10309-19.
HOTH, M. & PENNER, R. 1992. Depletion of intracellular calcium stores activates a calcium current in mast cells. *Nature,* 355**,** 353-6.
HOU, X., PEDI, L., DIVER, M. M. & LONG, S. B. 2012. Crystal structure of the calcium release-activated calcium channel Orai. *Science,* 338**,** 1308-13.
HUANG, X., LEI, Z. & EL-MALLAKH, R. S. 2007. Lithium normalizes elevated intracellular sodium. *Bipolar Disord,* 9**,** 298-300.
JI, W., XU, P., LI, Z., LU, J., LIU, L., ZHAN, Y., CHEN, Y., HILLE, B., XU, T. & CHEN, L. 2008. Functional stoichiometry of the unitary calcium-release-activated calcium channel. *Proc Natl Acad Sci U S A,* 105**,** 13668-73.
JOPE, R. S. 1999. A bimodal model of the mechanism of action of lithium. *Mol Psychiatry,* 4**,** 21-5.
JUNG, H. H., DANEK, A. & WALKER, R. H. 2011. Neuroacanthocytosis syndromes. *Orphanet J Rare Dis,* 6**,** 68.
KATAN, M. 1998. Families of phosphoinositide-specific phospholipase C: structure and function. *Biochim Biophys Acta,* 1436**,** 5-17.
KAWASAKI, T., LANGE, I. & FESKE, S. 2009. A minimal regulatory domain in the C terminus of STIM1 binds to and activates ORAI1 CRAC channels. *Biochem Biophys Res Commun,* 385**,** 49-54.
KIM, Y. H., RANE, A., LUSSIER, S. & ANDERSEN, J. K. 2011. Lithium protects against oxidative stress-mediated cell death in alpha-synuclein-overexpressing in vitro and in vivo models of Parkinson's disease. *J Neurosci Res,* 89**,** 1666-75.
KOCH, G. L. 1990. The endoplasmic reticulum and calcium storage. *Bioessays,* 12**,** 527-31.
KURANO, Y., NAKAMURA, M., ICHIBA, M., MATSUDA, M., MIZUNO, E., KATO, M., AGEMURA, A., IZUMO, S. & SANO, A. 2007. In vivo distribution and localization of chorein. *Biochem Biophys Res Commun,* 353**,** 431-5.
LAEMMLI, U. K. 1970. Cleavage of structural proteins during the assembly of the head of bacteriophage T4. *Nature,* 227**,** 680-5.
LANG, F., BOHMER, C., PALMADA, M., SEEBOHM, G., STRUTZ-SEEBOHM, N. & VALLON, V. 2006a. (Patho)physiological significance of the serum- and glucocorticoid-inducible kinase isoforms. *Physiol Rev,* 86**,** 1151-78.
LANG, F. & COHEN, P. 2001. Regulation and physiological roles of serum- and glucocorticoid-induced protein kinase isoforms. *Sci STKE,* 2001**,** re17.

LANG, F., EYLENSTEIN, A. & SHUMILINA, E. 2012. Regulation of Orai1/STIM1 by the kinases SGK1 and AMPK. *Cell Calcium,* 52**,** 347-54.
LANG, F. & HOFFMANN, E. K. 2012. Role of ion transport in control of apoptotic cell death. *Compr Physiol,* 2**,** 2037-61.
LANG, F., SHUMILINA, E., RITTER, M., GULBINS, E., VERENINOV, A. & HUBER, S. M. 2006b. Ion channels and cell volume in regulation of cell proliferation and apoptotic cell death. *Contrib Nephrol,* 152**,** 142-60.
LANG, F. & STOURNARAS, C. 2014. Ion channels in cancer: future perspectives and clinical potential. *Philos Trans R Soc Lond B Biol Sci,* 369**,** 20130108.
LAZZARA, C. A. & KIM, Y. H. 2015. Potential application of lithium in Parkinson's and other neurodegenerative diseases. *Front Neurosci,* 9**,** 403.
LI, Z., LU, J., XU, P., XIE, X., CHEN, L. & XU, T. 2007. Mapping the interacting domains of STIM1 and Orai1 in Ca2+ release-activated Ca2+ channel activation. *J Biol Chem,* 282**,** 29448-56.
LIOU, J., FIVAZ, M., INOUE, T. & MEYER, T. 2007. Live-cell imaging reveals sequential oligomerization and local plasma membrane targeting of stromal interaction molecule 1 after Ca2+ store depletion. *Proc Natl Acad Sci U S A,* 104**,** 9301-6.
LIOU, J., KIM, M. L., HEO, W. D., JONES, J. T., MYERS, J. W., FERRELL, J. E., JR. & MEYER, T. 2005. STIM is a Ca2+ sensor essential for Ca2+-store-depletion-triggered Ca2+ influx. *Curr Biol,* 15**,** 1235-41.
LUIK, R. M., WANG, B., PRAKRIYA, M., WU, M. M. & LEWIS, R. S. 2008. Oligomerization of STIM1 couples ER calcium depletion to CRAC channel activation. *Nature,* 454**,** 538-42.
MAURER, U., PREISS, F., BRAUNS-SCHUBERT, P., SCHLICHER, L. & CHARVET, C. 2014. GSK-3 - at the crossroads of cell death and survival. *J Cell Sci,* 127**,** 1369-78.
MCALLISTER, A. K., KATZ, L. C. & LO, D. C. 1999. Neurotrophins and synaptic plasticity. *Annu Rev Neurosci,* 22**,** 295-318.
MCNALLY, B. A., YAMASHITA, M., ENGH, A. & PRAKRIYA, M. 2009. Structural determinants of ion permeation in CRAC channels. *Proc Natl Acad Sci U S A,* 106**,** 22516-21.
MERCER, J. C., DEHAVEN, W. I., SMYTH, J. T., WEDEL, B., BOYLES, R. R., BIRD, G. S. & PUTNEY, J. W., JR. 2006. Large store-operated calcium selective currents due to co-expression of Orai1 or Orai2 with the intracellular calcium sensor, Stim1. *J Biol Chem,* 281**,** 24979-90.
MIGNEN, O., THOMPSON, J. L. & SHUTTLEWORTH, T. J. 2008. Orai1 subunit stoichiometry of the mammalian CRAC channel pore. *J Physiol,* 586**,** 419-25.
MOORADIAN, A. D. 1994. Potential mechanisms of the age-related changes in the blood-brain barrier. *Neurobiol Aging,* 15**,** 751-5; discussion 761-2, 767.
MUIK, M., FAHRNER, M., DERLER, I., SCHINDL, R., BERGSMANN, J., FRISCHAUF, I., GROSCHNER, K. & ROMANIN, C. 2009. A Cytosolic Homomerization and a Modulatory Domain within STIM1 C Terminus Determine Coupling to ORAI1 Channels. *J Biol Chem,* 284**,** 8421-6.
MUIK, M., FAHRNER, M., SCHINDL, R., STATHOPULOS, P., FRISCHAUF, I., DERLER, I., PLENK, P., LACKNER, B., GROSCHNER, K., IKURA, M. & ROMANIN, C. 2011. STIM1 couples to ORAI1 via an intramolecular transition into an extended conformation. *EMBO J,* 30**,** 1678-89.

MUIK, M., FRISCHAUF, I., DERLER, I., FAHRNER, M., BERGSMANN, J., EDER, P., SCHINDL, R., HESCH, C., POLZINGER, B., FRITSCH, R., KAHR, H., MADL, J., GRUBER, H., GROSCHNER, K. & ROMANIN, C. 2008. Dynamic coupling of the putative coiled-coil domain of ORAI1 with STIM1 mediates ORAI1 channel activation. *J Biol Chem,* 283**,** 8014-22.

MULLER-OERLINGHAUSEN, B. & LEWITZKA, U. 2010. Lithium reduces pathological aggression and suicidality: a mini-review. *Neuropsychobiology,* 62**,** 43-9.

MULLINS, F. M., PARK, C. Y., DOLMETSCH, R. E. & LEWIS, R. S. 2009. STIM1 and calmodulin interact with Orai1 to induce Ca2+-dependent inactivation of CRAC channels. *Proc Natl Acad Sci U S A,* 106**,** 15495-500.

NAMBUDIRI, D. E., MEYERS, B. S. & YOUNG, R. C. 1991. Delayed recovery from lithium neurotoxicity. *J Geriatr Psychiatry Neurol,* 4**,** 40-3.

OKITA, K., MATSUMURA, Y., SATO, Y., OKADA, A., MORIZANE, A., OKAMOTO, S., HONG, H., NAKAGAWA, M., TANABE, K., TEZUKA, K., SHIBATA, T., KUNISADA, T., TAKAHASHI, M., TAKAHASHI, J., SAJI, H. & YAMANAKA, S. 2011. A more efficient method to generate integration-free human iPS cells. *Nat Methods,* 8**,** 409-12.

ORRENIUS, S., ZHIVOTOVSKY, B. & NICOTERA, P. 2003. Regulation of cell death: the calcium-apoptosis link. *Nat Rev Mol Cell Biol,* 4**,** 552-65.

PACHET, A. K. & WISNIEWSKI, A. M. 2003. The effects of lithium on cognition: an updated review. *Psychopharmacology (Berl),* 170**,** 225-234.

PALTY, R., STANLEY, C. & ISACOFF, E. Y. 2015. Critical role for Orai1 C-terminal domain and TM4 in CRAC channel gating. *Cell Res,* 25**,** 963-80.

PAP, M. & COOPER, G. M. 1998. Role of glycogen synthase kinase-3 in the phosphatidylinositol 3-Kinase/Akt cell survival pathway. *J Biol Chem,* 273**,** 19929-32.

PARK, C. Y., HOOVER, P. J., MULLINS, F. M., BACHHAWAT, P., COVINGTON, E. D., RAUNSER, S., WALZ, T., GARCIA, K. C., DOLMETSCH, R. E. & LEWIS, R. S. 2009. STIM1 clusters and activates CRAC channels via direct binding of a cytosolic domain to Orai1. *Cell,* 136**,** 876-90.

PARKASH, J. & ASOTRA, K. 2010. Calcium wave signaling in cancer cells. *Life Sci,* 87**,** 587-95.

PARKER, N. J., BEGLEY, C. G., SMITH, P. J. & FOX, R. M. 1996. Molecular cloning of a novel human gene (D11S4896E) at chromosomal region 11p15.5. *Genomics,* 37**,** 253-6.

PEINELT, C., VIG, M., KOOMOA, D. L., BECK, A., NADLER, M. J., KOBLAN-HUBERSON, M., LIS, A., FLEIG, A., PENNER, R. & KINET, J. P. 2006. Amplification of CRAC current by STIM1 and CRACM1 (Orai1). *Nat Cell Biol,* 8**,** 771-3.

PELZL, L., ELSIR, B., SAHU, I., BISSINGER, R., SINGH, Y., SUKKAR, B., HONISCH, S., SCHOELS, L., JEMAA, M., LANG, E., STORCH, A., HERMANN, A., STOURNARAS, C. & LANG, F. 2017a. Lithium Sensitivity of Store Operated Ca2+ Entry and Survival of Fibroblasts Isolated from Chorea-Acanthocytosis Patients. *Cell Physiol Biochem,* 42**,** 2066-2077.

PELZL, L., HAUSER, S., ELSIR, B., SUKKAR, B., SAHU, I., SINGH, Y., HOFLINGER, P., BISSINGER, R., JEMAA, M., STOURNARAS, C., SCHOLS, L. & LANG, F. 2017b. Lithium Sensitive ORAI1 Expression, Store Operated

Ca(2+) Entry and Suicidal Death of Neurons in Chorea-Acanthocytosis. *Sci Rep,* 7**,** 6457.
PENNA, A., DEMURO, A., YEROMIN, A. V., ZHANG, S. L., SAFRINA, O., PARKER, I. & CAHALAN, M. D. 2008. The CRAC channel consists of a tetramer formed by Stim-induced dimerization of Orai dimers. *Nature,* 456**,** 116-20.
PLATMAN, S. R. & FIEVE, R. R. 1968. Biochemical aspects of lithium in affective disorders. *Arch Gen Psychiatry,* 19**,** 659-63.
POLGAR, J., CHUNG, S. H. & REED, G. L. 2002. Vesicle-associated membrane protein 3 (VAMP-3) and VAMP-8 are present in human platelets and are required for granule secretion. *Blood,* 100**,** 1081-3.
PRAKRIYA, M., FESKE, S., GWACK, Y., SRIKANTH, S., RAO, A. & HOGAN, P. G. 2006. Orai1 is an essential pore subunit of the CRAC channel. *Nature,* 443**,** 230-3.
PREVARSKAYA, N., OUADID-AHIDOUCH, H., SKRYMA, R. & SHUBA, Y. 2014. Remodelling of Ca2+ transport in cancer: how it contributes to cancer hallmarks? *Philos Trans R Soc Lond B Biol Sci,* 369**,** 20130097.
PREVARSKAYA, N., SKRYMA, R. & SHUBA, Y. 2011. Calcium in tumour metastasis: new roles for known actors. *Nat Rev Cancer,* 11**,** 609-18.
PUTNEY, J. W., JR. 1986. A model for receptor-regulated calcium entry. *Cell Calcium,* 7**,** 1-12.
PUTNEY, J. W., JR. 2007. New molecular players in capacitative Ca2+ entry. *J Cell Sci,* 120**,** 1959-65.
PUTNEY, J. W. & TOMITA, T. 2012. Phospholipase C signaling and calcium influx. *Adv Biol Regul,* 52**,** 152-64.
QU, B., AL-ANSARY, D., KUMMEROW, C., HOTH, M. & SCHWARZ, E. C. 2011. ORAI-mediated calcium influx in T cell proliferation, apoptosis and tolerance. *Cell Calcium,* 50**,** 261-9.
RAIMONDI, C. & FALASCA, M. 2011. Targeting PDK1 in cancer. *Curr Med Chem,* 18**,** 2763-9.
RAMPOLDI, L., DANEK, A. & MONACO, A. P. 2002. Clinical features and molecular bases of neuroacanthocytosis. *J Mol Med (Berl),* 80**,** 475-91.
RAMPOLDI, L., DOBSON-STONE, C., RUBIO, J. P., DANEK, A., CHALMERS, R. M., WOOD, N. W., VERELLEN, C., FERRER, X., MALANDRINI, A., FABRIZI, G. M., BROWN, R., VANCE, J., PERICAK-VANCE, M., RUDOLF, G., CARRE, S., ALONSO, E., MANFREDI, M., NEMETH, A. H. & MONACO, A. P. 2001. A conserved sorting-associated protein is mutant in chorea-acanthocytosis. *Nat Genet,* 28**,** 119-20.
REUTELINGSPERGER, C. P. & VAN HEERDE, W. L. 1997. Annexin V, the regulator of phosphatidylserine-catalyzed inflammation and coagulation during apoptosis. *Cell Mol Life Sci,* 53**,** 527-32.
RHEE, S. G. & BAE, Y. S. 1997. Regulation of phosphoinositide-specific phospholipase C isozymes. *J Biol Chem,* 272**,** 15045-8.
ROOS, J., DIGREGORIO, P. J., YEROMIN, A. V., OHLSEN, K., LIOUDYNO, M., ZHANG, S., SAFRINA, O., KOZAK, J. A., WAGNER, S. L., CAHALAN, M. D., VELICELEBI, G. & STAUDERMAN, K. A. 2005. STIM1, an essential and conserved component of store-operated Ca2+ channel function. *J Cell Biol,* 169**,** 435-45.
SAIKI, S., SAKAI, K., MURATA, K. Y., SAIKI, M., NAKANISHI, M., KITAGAWA, Y., KAITO, M., GONDO, Y., KUMAMOTO, T., MATSUI, M., HATTORI, N. &

HIROSE, G. 2007. Primary skeletal muscle involvement in chorea-acanthocytosis. *Mov Disord,* 22**,** 848-52.
SCHARENBERG, A. M. & KINET, J. P. 1998. PtdIns-3,4,5-P3: a regulatory nexus between tyrosine kinases and sustained calcium signals. *Cell,* 94**,** 5-8.
SCHEID, R., BADER, B., OTT, D. V., MERKENSCHLAGER, A. & DANEK, A. 2009. Development of mesial temporal lobe epilepsy in chorea-acanthocytosis. *Neurology,* 73**,** 1419-22.
SCHMIDT, E. M., SCHMID, E., MUNZER, P., HERMANN, A., EYRICH, A. K., RUSSO, A., WALKER, B., GU, S., VOM HAGEN, J. M., FAGGIO, C., SCHALLER, M., FOLLER, M., SCHOLS, L., GAWAZ, M., BORST, O., STORCH, A., STOURNARAS, C. & LANG, F. 2013. Chorein sensitivity of cytoskeletal organization and degranulation of platelets. *FASEB J,* 27**,** 2799-806.
SCHMIDT, S., LIU, G., LIU, G., YANG, W., HONISCH, S., PANTELAKOS, S., STOURNARAS, C., HONIG, A. & LANG, F. 2014. Enhanced Orai1 and STIM1 expression as well as store operated Ca2+ entry in therapy resistant ovary carcinoma cells. *Oncotarget,* 5**,** 4799-810.
SCHNEIDER, S. A., AGGARWAL, A., BHATT, M., DUPONT, E., TISCH, S., LIMOUSIN, P., LEE, P., QUINN, N. & BHATIA, K. P. 2006. Severe tongue protrusion dystonia: clinical syndromes and possible treatment. *Neurology,* 67**,** 940-3.
SCHOU, M. 1957. Biology and pharmacology of the lithium ion. *Pharmacol Rev,* 9**,** 17-58.
SHEARD, M. H., MARINI, J. L., BRIDGES, C. I. & WAGNER, E. 1976. The effect of lithium on impulsive aggressive behavior in man. *Am J Psychiatry,* 133**,** 1409-13.
SHI, Y., KIRWAN, P. & LIVESEY, F. J. 2012. Directed differentiation of human pluripotent stem cells to cerebral cortex neurons and neural networks. *Nat Protoc,* 7**,** 1836-46.
SIEBENLIST, U., FRANZOSO, G. & BROWN, K. 1994. Structure, regulation and function of NF-kappa B. *Annu Rev Cell Biol,* 10**,** 405-55.
SOBOLOFF, J., SPASSOVA, M. A., TANG, X. D., HEWAVITHARANA, T., XU, W. & GILL, D. L. 2006. Orai1 and STIM reconstitute store-operated calcium channel function. *J Biol Chem,* 281**,** 20661-5.
SOMASUNDARAM, A., SHUM, A. K., MCBRIDE, H. J., KESSLER, J. A., FESKE, S., MILLER, R. J. & PRAKRIYA, M. 2014. Store-operated CRAC channels regulate gene expression and proliferation in neural progenitor cells. *J Neurosci,* 34**,** 9107-23.
SPROULE, B. A., HARDY, B. G. & SHULMAN, K. I. 2000. Differential pharmacokinetics of lithium in elderly patients. *Drugs Aging,* 16**,** 165-77.
STAMBOLIC, V., RUEL, L. & WOODGETT, J. R. 1996. Lithium inhibits glycogen synthase kinase-3 activity and mimics wingless signalling in intact cells. *Curr Biol,* 6**,** 1664-8.
STATHOPULOS, P. B., LI, G. Y., PLEVIN, M. J., AMES, J. B. & IKURA, M. 2006. Stored Ca2+ depletion-induced oligomerization of stromal interaction molecule 1 (STIM1) via the EF-SAM region: An initiation mechanism for capacitive Ca2+ entry. *J Biol Chem,* 281**,** 35855-62.
SUKKAR, B., HAUSER, S., PELZL, L., HOSSEINZADEH, Z., SAHU, I., AL-MAGHOUT, T., BHUYAN, A. A. M., ZACHAROPOULOU, N., STOURNARAS,

C., SCHOLS, L. & LANG, F. 2018. Inhibition of Lithium Sensitive Orai1/ STIM1 Expression and Store Operated Ca2+ Entry in Chorea-Acanthocytosis Neurons by NF-kappaB Inhibitor Wogonin. *Cell Physiol Biochem,* 51**,** 278-289.

TAKEMURA, H., HUGHES, A. R., THASTRUP, O. & PUTNEY, J. W., JR. 1989. Activation of calcium entry by the tumor promoter thapsigargin in parotid acinar cells. Evidence that an intracellular calcium pool and not an inositol phosphate regulates calcium fluxes at the plasma membrane. *J Biol Chem,* 264**,** 12266-71.

TAYLOR, J. T., ZENG, X. B., POTTLE, J. E., LEE, K., WANG, A. R., YI, S. G., SCRUGGS, J. A., SIKKA, S. S. & LI, M. 2008. Calcium signaling and T-type calcium channels in cancer cell cycling. *World J Gastroenterol,* 14**,** 4984-91.

UENO, S., MARUKI, Y., NAKAMURA, M., TOMEMORI, Y., KAMAE, K., TANABE, H., YAMASHITA, Y., MATSUDA, S., KANEKO, S. & SANO, A. 2001. The gene encoding a newly discovered protein, chorein, is mutated in chorea-acanthocytosis. *Nat Genet,* 28**,** 121-2.

VANHAESEBROECK, B., STEPHENS, L. & HAWKINS, P. 2012. PI3K signalling: the path to discovery and understanding. *Nat Rev Mol Cell Biol,* 13**,** 195-203.

VELAYOS-BAEZA, A., VETTORI, A., COPLEY, R. R., DOBSON-STONE, C. & MONACO, A. P. 2004. Analysis of the human VPS13 gene family. *Genomics,* 84**,** 536-49.

VELAYOS BAEZA, A., DOBSON-STONE, C., RAMPOLDI, L., BADER, B., WALKER, R. H., DANEK, A. & MONACO, A. P. 1993. Chorea-Acanthocytosis. *In:* ADAM, M. P., ARDINGER, H. H., PAGON, R. A., WALLACE, S. E., BEAN, L. J. H., STEPHENS, K. & AMEMIYA, A. (eds.) *GeneReviews((R)).* Seattle (WA).

VIG, M., BECK, A., BILLINGSLEY, J. M., LIS, A., PARVEZ, S., PEINELT, C., KOOMOA, D. L., SOBOLOFF, J., GILL, D. L., FLEIG, A., KINET, J. P. & PENNER, R. 2006a. CRACM1 multimers form the ion-selective pore of the CRAC channel. *Curr Biol,* 16**,** 2073-9.

VIG, M., PEINELT, C., BECK, A., KOOMOA, D. L., RABAH, D., KOBLAN-HUBERSON, M., KRAFT, S., TURNER, H., FLEIG, A., PENNER, R. & KINET, J. P. 2006b. CRACM1 is a plasma membrane protein essential for store-operated Ca2+ entry. *Science,* 312**,** 1220-3.

WALKER, R. H. 2015. Untangling the Thorns: Advances in the Neuroacanthocytosis Syndromes. *J Mov Disord,* 8**,** 41-54.

WATASE, K., GATCHEL, J. R., SUN, Y., EMAMIAN, E., ATKINSON, R., RICHMAN, R., MIZUSAWA, H., ORR, H. T., SHAW, C. & ZOGHBI, H. Y. 2007. Lithium therapy improves neurological function and hippocampal dendritic arborization in a spinocerebellar ataxia type 1 mouse model. *PLoS Med,* 4**,** e182.

WU, C., MA, M. H., BROWN, K. R., GEISLER, M., LI, L., TZENG, E., JIA, C. Y., JURISICA, I. & LI, S. S. 2007. Systematic identification of SH3 domain-mediated human protein-protein interactions by peptide array target screening. *Proteomics,* 7**,** 1775-85.

WU, M. M., BUCHANAN, J., LUIK, R. M. & LEWIS, R. S. 2006. Ca2+ store depletion causes STIM1 to accumulate in ER regions closely associated with the plasma membrane. *J Cell Biol,* 174**,** 803-13.

YOUDIM, M. B. & ARRAF, Z. 2004. Prevention of MPTP (N-methyl-4-phenyl-1,2,3,6-tetrahydropyridine) dopaminergic neurotoxicity in mice by chronic lithium: involvements of Bcl-2 and Bax. *Neuropharmacology,* 46**,** 1130-40.

YUAN, J. P., ZENG, W., DORWART, M. R., CHOI, Y. J., WORLEY, P. F. & MUALLEM, S. 2009. SOAR and the polybasic STIM1 domains gate and regulate Orai channels. *Nat Cell Biol,* 11**,** 337-43.

ZHANG, L., CUI, R., CHENG, X. & DU, J. 2005a. Antiapoptotic effect of serum and glucocorticoid-inducible protein kinase is mediated by novel mechanism activating I{kappa}B kinase. *Cancer Res,* 65**,** 457-64.

ZHANG, L., WANG, S. & LIN, J. 2013. Clinical and molecular research of neuroacanthocytosis. *Neural Regen Res,* 8**,** 833-42.

ZHANG, S. L., YEROMIN, A. V., ZHANG, X. H., YU, Y., SAFRINA, O., PENNA, A., ROOS, J., STAUDERMAN, K. A. & CAHALAN, M. D. 2006. Genome-wide RNAi screen of Ca(2+) influx identifies genes that regulate Ca(2+) release-activated Ca(2+) channel activity. *Proc Natl Acad Sci U S A,* 103**,** 9357-62.

ZHANG, S. L., YU, Y., ROOS, J., KOZAK, J. A., DEERINCK, T. J., ELLISMAN, M. H., STAUDERMAN, K. A. & CAHALAN, M. D. 2005b. STIM1 is a Ca2+ sensor that activates CRAC channels and migrates from the Ca2+ store to the plasma membrane. *Nature,* 437**,** 902-5.

ZHAO, Q., WANG, J., ZOU, M. J., HU, R., ZHAO, L., QIANG, L., RONG, J. J., YOU, Q. D. & GUO, Q. L. 2010. Wogonin potentiates the antitumor effects of low dose 5-fluorouracil against gastric cancer through induction of apoptosis by down-regulation of NF-kappaB and regulation of its metabolism. *Toxicol Lett,* 197**,** 201-10.

ZHOU, Y., RAMACHANDRAN, S., OH-HORA, M., RAO, A. & HOGAN, P. G. 2010. Pore architecture of the ORAI1 store-operated calcium channel. *Proc Natl Acad Sci U S A,* 107**,** 4896-901.

8. Declaration of contributions

I assure that the submitted work has not been submitted previously or used by another examination authority for the purpose of a doctoral or other examination procedure and is all written by me, and all the used sources are cited properly.

Stefan Hauser, Alexander Storch, Andreas Hermann and Philip Höflinger provided the cells that were used in this study.

Ca^{2+} measurement experiments were carried out by me, Lisann Pelzl and Tamer Al-Maghout.

qPCR experiments were carried out by me and Itishri Sahu.

Western blot experiments were carried out by me.

Bhaeldin Elsir, Abdulla Al Mamun Bhuyan, Rosi Bissinger, Yogesh Singh, Mohamed Jemaà and Elisabeth Lang carried out flow cytometry experiments.

Florian Lang, Christos Stournaras and Ludger Schoels designed the study.

The work in this thesis has been published:

Inhibition of Lithium Sensitive ORAI1/ STIM1 Expression and Store Operated Ca2+ Entry in Chorea-Acanthocytosis Neurons by NF-κB Inhibitor Wogonin.

Basma Sukkar, Stefan Hauser, Lisann Pelzl, Zohreh Hosseinzadeh, Itishri Sahu, Tamer al-Maghout, Abdulla Al Mamun Bhuyan, Nefeli Zacharopoulou, Christos Stournaras Ludger Schöls and Florian Lang. Cell Physiol Biochem. 2018;51(1):278-289. doi: 10.1159/000495229. Epub 2018 Nov 19. PMID: 30453283 (Sukkar et al., 2018).

Lithium Sensitivity of Store Operated Ca2+ Entry and Survival of Fibroblasts Isolated from Chorea-Acanthocytosis Patients.

Lisann Pelzl, Bhaeldin Elsir, Itishri Sahu, Rosi Bissinger, Yogesh Singh, Basma Sukkar, Sabina Honisch, Ludger Schoels, Mohamed Jemaà, Elisabeth Lang, Alexander Storch, Andreas Hermann, Christos Stournaras and Florian Lang. Cell Physiol Biochem. 2017;42(5):2066-2077. doi: 10.1159/000479901. Epub 2017 Aug 11. PMID: 28803243 (Pelzl et al., 2017a).

Lithium Sensitive ORAI1 Expression, Store Operated Ca2+ Entry and Suicidal Death of Neurons in Chorea-Acanthocytosis.

Lisann Pelzl, Stefan Hauser, Bhaeldin Elsir, Basma Sukkar, Itishri Sahu, Yogesh Singh, Philip Höflinger, Rosi Bissinger, Mohamed Jemaà, Christos Stournaras, Ludger Schöls and Florian Lang. Sci Rep. 2017 Jul 25;7(1):6457. doi: 10.1038/s41598-017-06451-1. PMID: 28743945 (Pelzl et al., 2017b).

The author

Basma Sukkar

List of Publications

1. Pelzl L, Sahu I, Ma K, Heinzmann D, Bhuyan AAM, Al-Maghout T, **Sukkar B**, Sharma Y, Marini I, Rigoni F, Artunc F, Cao H, Gutti R, Voelkl J, Pieske B, Gawaz M, Bakchoul T, Lang F. "Beta-Glycerophosphate-Induced ORAI1 Expression and Store Operated Ca^{2+} Entry in Megakaryocytes." *Sci Rep.* Epub 2020 Feb 3. PMID: 32015442.
2. Abdelazeem KNM, Droppova B, **Sukkar B**, Al-Maghout T, Pelzl L, Zacharopoulou N, Ali Hassan NH, Abdel-Fattah KI, Stournaras C, Lang F. "Upregulation of Orai1 and STIM1 expression as well as store-operated Ca2+ entry in ovary carcinoma cells by placental growth factor.'' *Biochem Biophys Res Commun.* Epub 2019 Mar 20. PMID: 30902388.
3. **Sukkar B**, Hauser S, Pelzl L, Hosseinzadeh Z, Sahu I, Al-Maghout T, Bhuyan AAM, Zacharopoulou N, Stournaras C, Schöls L, Lang F. "Inhibition of Lithium Sensitive ORAI1/ STIM1 Expression and Store Operated Ca2+ Entry in Chorea-Acanthocytosis Neurons by NF-κB Inhibitor Wogonin.'' *Cell Physiol Biochem*. Epub 2018 Nov 19. PMID: 30453283.
4. Bissinger R, Lang E, Gonzalez-Menendez I, Quintanilla-Martinez L, Ghashghaeinia M, Pelzl L, **Sukkar B**, Bhuyan AAM, Salker MS, Singh Y, Fehrenbacher B, Fakhri H, Umbach AT, Schaller M, Qadri SM, Lang F. "Genetic deficiency of the tumor suppressor protein p53 influences erythrocyte survival''. *Apoptosis*. 2018 Dec 23. PMID: 30238335.
5. Pelzl L, Elsir B, Sahu I, Bissinger R, Singh Y, **Sukkar B**, Honisch S, Schoels L, Jemaà M, Lang E, Storch A, Hermann A, Stournaras C, Lang F. "Lithium Sensitivity of Store Operated Ca2+ Entry and Survival of Fibroblasts Isolated from Chorea-Acanthocytosis Patients''. *Cell Physiol Biochem*. Epub 2017 Aug 11. PMID: 28803243.
6. Pelzl L, Hauser S, Elsir B, **Sukkar B**, Sahu I, Singh Y, Höflinger P, Bissinger R, Jemaà M, Stournaras C, Schöls L, Lang F. "Lithium Sensitive ORAI1 Expression, Store Operated Ca2+ Entry and Suicidal Death of Neurons in Chorea-Acanthocytosis''. *Sci Rep*. 2017 Jul 25. PMID: 28743945.
7. Sahu I, Pelzl L, **Sukkar B**, Fakhri H, Al-Maghout T, Cao H, Hauser S, Gutti R, Gawaz M, Lang F. "NFAT5-sensitive ORAI1 expression and store-operated Ca2+ entry in megakaryocytes''. *FASEB J*. Epub 2017 Apr 26. PMID: 28446591.